Pergamon

Tetrahedron, Vol. 53, No. 30, pp. 10409-10432, 1997

0040-4020/97 $17.00 + 0.00

PII: S0040-4020(97)00631-5

Synthesis of 5'-Polyarene-Tethered Oligo-DNAs and the Thermal Stability and Spectroscopic Properties of Their Duplexes and Triplexes

Nitin Puri, Edouard Zamaratski, Christian Sund and Jyoti Chattopadhyaya*

Department of Bioorganic Chemistry, Box 581, Biomedical Center,
University of Uppsala, S-751 23 Uppsala, Sweden

E-mail: jyoti@bioorgchem.uu.se. Fax: +4618-554495

Abstract: Eleven different planar hydroxy alkylated polyarenes **1-11** with different geometry, bulk and electronic characteristics were synthesised, and used for tethering to the 5'-phosphate of a 9-mer and a 18-mer DNA sequences through solid-phase synthesis. The 5'-polyarene-tethered 9-mers **30-40** were tested for their ability to form stable duplexes with four complementary target DNA-strands **25-28** of different length. The 5'-polyarene-tethered 18-mers **44-54** were tested for their ability to form stable triplexes with a 24-mer duplex target **41+42**. The T_m measurements of duplexes at low salt and pH 7.3 showed that the angular nitro phenanthrene and phenanthrene conjugates **31** and **30** gave the highest duplex stabilisations with targets **25** (ΔT_m 13.8° C and 11.8° C) and **26** (ΔT_m 12.3° C and 11.9° C). With the mismatch sequence **28**, only **30** and **31** gave a high ΔT_m of 11.6° C and 10.8° C respectively, while lower ΔT_m values were observed for other conjugates (ΔT_m ~4.0-5.0° C). The T_m measurements of triplexes between **43-54** and duplex target **41+42** at low salt and pH 7.3, 6.5 and 6.0 without Mg^{2+} showed that the nitro phenanthrene conjugate **45** gave the best triplex stabilisation (ΔT_m 4.1-5.4° C). The stabilisation of nitro phenanthrene conjugate **45** compared to phenanthrene conjugate **44** increased more remarkably when Mg^{2+} was present: **45** (ΔT_m 15° C), **44** (ΔT_m 10° C). These results imply that the electron density of the chromophore influences the π-π stacking interactions between the chromophore and nucleobases, and thereby influencing the duplex and triplex stability. Fluorescence measurements on single strand to double strand transition indicated that the 5'-tethered polyarenes are stacked only on the neighbouring nucleobases of the opposite strand. In case of 5'-9-*N*-ethylphenazinium conjugate **36**, a comparative NMR and fluorescence measurement has unambiguously shown that the tethered phenazinium ion is indeed intercalated between the nucleotides of the opposite target strand **26**. Thermodynamic calculations showed the most stable ΔG°(298K) for **30**, **31**(+targets **25**, **26**, **28**) and **35**, **36**(+targets **25**, **26**) compared to the blank **29** ($\Delta\Delta G^{\circ}$(298K)~-10kJ mol^{-1}). The non-palindromic target **27** was shown by T_m measurements to form a stable tertiary structure, which was very little affected by addition of any 5'-tethered conjugate, thereby showing the importance of the tertiary structures of an *in vivo* antisense target and its implication in regard to its bioavailablity to complementary antisense probes.

Oligo-DNA conjugates are found to be potentially important because of their ability to act as repressors at the transcriptional (antigene) and translational (antisense) level of gene expression.[1a-d] For the effective design of these antisense or antigene agents, attempts are being made mainly to strengthen the Watson-Crick or Hoogsteen basepairing during hybridisation with complementary single- or double-stranded target nucleic acid. Improved duplex and triplex stabilisation has been achieved by derivatising the internucleotide phosphate linkages[2a,b,c] or by substituting it with various internucleoside aliphatic linkers,[1d, 2a,b,c] as well as by tethering

various kinds of ligands to the oligo-DNA probes at various sites.[2a,b,c] In the latter case, the ligands have been mostly planar polycyclic aromatic chromophores,[3a-c] alkyl groups[4a,b,c] and polyamines.[5a-f] These ligands have most commonly been tethered to the oligo-DNA through the 5'-end phosphate, 3'(2')-end phosphate, an internal phosphate, through a nucleobase, or directly through a sugar residue.

We have recently used high-field NMR spectroscopy for understanding the structural and mechanistic basis of stabilisation of both matched and mismatched oligo-DNA duplexes in which one of the strands was tethered with 5'-[*N*-(2-hydroxyethyl)phenazinium ion].[6] The NMR-constrained stereochemical model resulting from this study[6] showed that the 5'-tethered *N*-(2-hydroxyethyl)phenazinium ion was indeed intercalated between two nucleobases in the opposite stand, causing an increase of the T_m compared to the non-tethered natural counterpart. Thus, the 5'-tethered chromophore towards the end of the duplex intercalate between the nucleobases in the opposite strand easily, and stack more efficiently,[6] because of the poorer conformational rigidity of the terminal basepairs (weaker hydrogen bonding) compared to the core part of the duplex.

It has been shown that the surface area, electrostatics, polarisability and hydrophobicity of a tethered chromophore are the factors that dictate the strength of the π-stacking interactions in aqueous solutions.[7] Furthermore, titration studies of 9-ethyladenine with small synthetic receptors showed that the recognition elements within the receptors, which are focused on the purine nucleus, involve a combination of hydrogen bonding and "aryl stacking forces".[8] Clearly, the stability of the complex is being influenced by the specific electronic properties of the polycyclic aromatic "bottom" of the receptor.

In view of these studies, we decided to synthesise a series of planar polycyclic aromatic hydroxy alkylated chromophores with different geometry, bulk, electron density, polarisability as well as hydrophobicity, and tether them directly to the 5'-end of the single-stranded oligo-DNAs. Our objective was to determine whether the changes in the above factors of the 5'-tethered chromophore may be correlated to the melting temperatures (T_m), free energy ($\Delta G°$) and fluorescence properties of the duplexes and triplexes. Additionally, we also wanted to investigate how the nature of the target sequences (chain length, matched/mismatched basepairs at the chromophore stacking site and secondary structures) influences these physico-chemical properties of the duplexes and triplexes, in the light of our previous investigations.[6]

RESULTS AND DISCUSSION

(A) Synthesis of 5'-chromophore-tethered 9-mers ***30-40*** *for the duplex studies and the pyrimidine-rich 18-mers* ***43 - 54*** *for the triplex studies.*

In order to meet the above objectives, we prepared the 5'-chromophore-tethered thymidine 3'-phosphoramidite blocks **14c-17c**, **19c-22c**,[9] the corresponding 3'-phosphomonotriazolide **18c** (*in situ*)[10] and the chromophore linker phosphoramidites **23** and **24**, and used them in solid-phase synthesis[11a,b] of the mix-sequenced 5'-chromophore-tethered 9-mers **30-40** for the duplex studies and the pyrimidine-rich 18-mers **43 - 54** for the triplex studies. For the duplex studies, target sequences **25** (10-mer), **26** (11-mer), **27** (20-mer fully matched) and **28** (20-mer one basepair mismatched) were synthesised and for the triplex studies, the two complementary target sequences **42** (24-mer purine-rich) and **41** (24-mer pyrimidine-rich) were synthesised through solid-phase synthesis.

The hydroxyalkyl chromophores **1-11** were synthesised. The ethyl (-Y-CH_2CH_2-OP; Y = Me-N or O) linker between the chromophore and the 5'-phosphate (Fig. 1) was mainly used because this has been found to

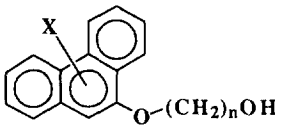

1: X = H, n = 2
2: X = NO_2, n = 2
3: X = H, n = 4

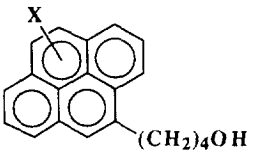

4: X = H
5: X = NO_2

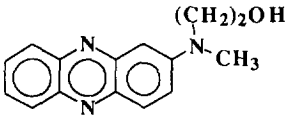

6

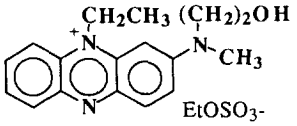

7

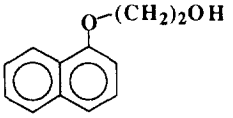

8

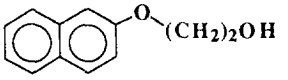

9

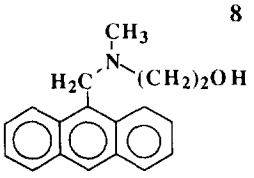

10

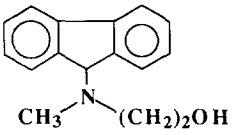

11

(A) Single strand targets for duplex formation

25: 5'-d(C<u>A T G T T T G G A</u>)-3' (10-mer)
26: 5'-d(C<u>A T G T T T G G A</u>C)-3' (11-mer)
27: 5'-d(TTAAC<u>A T G T T T G G A</u>CAAGTT)3' (matched 20-mer)
28: 5'-d(TTAAC<u>A T G T T T G G C</u>CAAGTT)-3' (mismatched 20-mer)

(B) Duplex target for triplex formation

41: 5'-d(G C G <u>T C T T T T T T C T T T T T T C T T</u> G G C)-3' (24-mer)
42: 3'-d(C G C <u>A G AA AA A A GA A AAA A G A A</u> C C G)-5' (24-mer)

(C) Non-tethered oligos

29: 3'-d(<u>T A C A A A C C T</u>)-5' (9-mer)
43: 3'-d(<u>T C T T T T T T C T T T T T T C T T</u>)-5' (18-mer)

(D) Nonamer conjugate **30-40**: 3'-d(<u>T A C A A A C C T</u>)-5'-$OP(O_2)^-$-**X**)

(E) Octadecamer conjugate **44-54**: 3'-d(<u>T C T T T T T T C T T T T T T C T T</u>)-5'-$OP(O_2)^-$-**X**)

(X = corresponding alkoxy moiety of the alcohols **1-11**)

30 & **44**: X = (**1**)
31 & **45**: X = (**2**)
32 & **46**: X = (**3**)
33 & **47**: X = (**4**)
34 & **48**: X = (**5**)
35 & **49**: X = (**6**)
36 & **50**: X = (**7**)
37 & **51**: X = (**8**)
38 & **52**: X = (**9**)
39 & **53**: X = (**10**)
40 & **54**: X = (**11**)

Fig. 1

Table 1 : The thermal stability of duplexes (T_m in °C) resulting from a 1:1 mixture of nonamer conjugates **29-40** with the targets **25, 26, 27 & 28.***

Entry#	9-mer conjugates 5'-X-$(CH_2)_n$OP(O_2)-O-TCCAAACAT-3'	10-mer target 5'-dCATGTTTGGA **25**		11-mer target 5'dCATGTTTGGAC **26**		20-mer target (matched) 5'-dTTAACATGTTTGGACAAGTT-3' **27**		20-mer target (mismatched) 5'-TTAACATGTTTGGCCAAGTT-3' **28**	
		T_m	ΔT_m	T_m	ΔT_m	T_m	ΔT_m	T_m	ΔT_m
1	**29**	26.2	-	25.9	-	37.7	-	24.0	-
2	**30**	38.0	11.8	37.8	11.9	38.1	0.4	35.6	11.6
3	**31**	40.0	13.8	38.2	12.3	38.0	0.3	36.2	12.2
4	**32**	33.4	7.2	34.2	8.3	36.7	-1.0	28.9	4.9
5	**33**	35.1	8.9	34.0	8.1	37.0	-0.5	30.6	6.6
6	**34**	33.7	7.5	32.2	6.3	38.7	1.0	27.9	3.9
7	**35**	37.7	11.5	35.9	10.0	38.1	0.6	27.8	3.8
8	**36**	36.5	10.3	38.1	12.2	38.6	0.9	28.7	4.7
9	**37**	32.3	6.1	31.0	5.1	37.4	-0.3	29.5	5.5
10	**38**	32.8	6.6	32.5	6.6	37.8	0.1	28.5	4.5
11	**39**	33.0	6.8	33.9	8.0	39.6	1.9	28.1	4.6
12	**40**	31.0	4.8	30.2	4.3	38.2	0.5	26.8	2.8

* The protocol for measuring the T_m of the duplexes is reported in the experimentals.

be the optimised length in case of 5'-[*N*-(2-hydroxyethyl)phenazinium]-tethered oligo-DNAs.[12]

For the syntheses of 9-(2-hydroxyethoxy)phenanthrene (**1**) (54%), 9-(4-hydroxybutoxy)phenanthrene (**3**) (34%), 1-(2-hydroxyethoxy)naphthalene (**8**) (60%) and 2-(2-hydroxyethoxy)naphthalene (**9**) (72%), the corresponding commercially available polycyclic phenols were alkylated using 1-*O*-MMTr-$(CH_2)_n$-CH_2-Cl (n = 1 or 3), under basic conditions, followed by acid treatment to remove the MMTr-protecting group.

For the synthesis of 2-[(*N*-(2-hydroxyethyl)-*N*-methyl)amino]-9-*N*-ethylphenazinium ethylsulphate (**7**) (44%), modified protocols of earlier reports were used,[12a,b] starting with 9-*N*-ethylation of phenazine and subsequent coupling with 2-(*N*-methylamino)ethanol.

For the synthesis of 2-(*N*-(2-hydroxyethyl)-*N*-methyl)aminophenazine (**6**) (28%), 9-*N*-methylation of phenazine[13] was carried out instead, and after coupling with 2-(*N*-methylamino)ethanol, the 9-*N*-methyl group from the phenazinium derivative was removed by aqueous ammonia treatment.

9-(*N*-(2-hydroxyethyl)-*N*-methyl) aminomethyl anthracene (**10**) (80%) and 9-(*N*-(2-hydroxyethyl)-*N*-methyl)amino fluorene (**11**) (80%) were synthesised through a simple aliphatic substitution reaction of 9-(chloromethyl)anthracene and 9-bromofluorene, respectively, with 2-(*N*-methylamino)ethanol. Nitration of **1** and 4-(pyren-1-yl)butanol (**4**) was carried out under mild conditions according to known procedures,[14] giving exclusively the corresponding mono nitrated products **2** (90%) and **5** (95%), each one as an intractable mixture of three different mononitro isomers.

The hydroxy alkylated chromophores **1-3**, **6-11** were used in a three-step synthesis of the corresponding protected 5'-chromophore-tethered 3'-phosphoramidite blocks **14c-17c** and **19c-22c**, which were used in standard solid-phase synthesis[11b] of the 5'-chromophore-tethered oligonucleotides **30-40** and **44-54**.

Standard protocols were used for the (i) condensation of chromophores **1-3** and **6-11** with the 5'-phosphoramidite blocks **12** or **13**[9] (Fig. 2) to give **14a-22a** (45-92%) (ii) for the depixylation of blocks **14a-22a** to **14b-22b**[15a,b] (56-86%), and (iii) for the synthesis of the phosphoramidite blocks **14c-17c** (65-86%), **19c-22c**[11a] (53-80%). Block **18b** was phosphorylated by *o*-chlorophenylphosphoro-bis-triazolide,[16] and then directly coupled[10] to CPG-bound 5'-hydroxyoctamer analogue of 9-mer **29** [5'-d(CCAAACAT)-CPG for synthesis of **36**] and to CPG-bound 5'-hydroxyheptadecamer analogue of 18-mer **43** [5'-d(TCT_6CT_6CT)-CPG for synthesis of **50**].

Tethering of chromophores **1-11** to oligonucleotides using the above approach gave direct access to the fully deprotected 5'-(chromophore alkyl) phosphothymidine monomer blocks for our fluorescence measurements, but this approach also circumvented stability and purification problems that arose when a direct phosphitylation of **7**, **10** and **11** was attempted. However, compounds **4** and **5** were directly converted in the standard way to the corresponding phosphoramidites **23** and **24**, which were used for the solid-phase preparation of 5'-tethered oligonucleotides **33**, **34**, **47** and **48**, and for the solid-phase preparation of the monomeric 5'-(4-(pyren-1-yl)butyl)phosphothymidine and 5'-(4-(mono nitro pyren-1-yl)butyl)phosphothymidine blocks.

Synthesis, deprotection and purification of oligonucleotides **25-54** are described in the experimental section. The hplc profiles (not shown) of the purified sodium exchanged oligomers revealed that tethering of the hydroxy alkylated chromophores **1-11** to the 5'-end of nonamer **29** and octadecamer **43** gave strongly retarded retention times (R_t) compared to the corresponding underivatized oligomer, the nonamer conjugates having expectedly longer R_ts than the corresponding octadecamer conjugates (see experimentals).

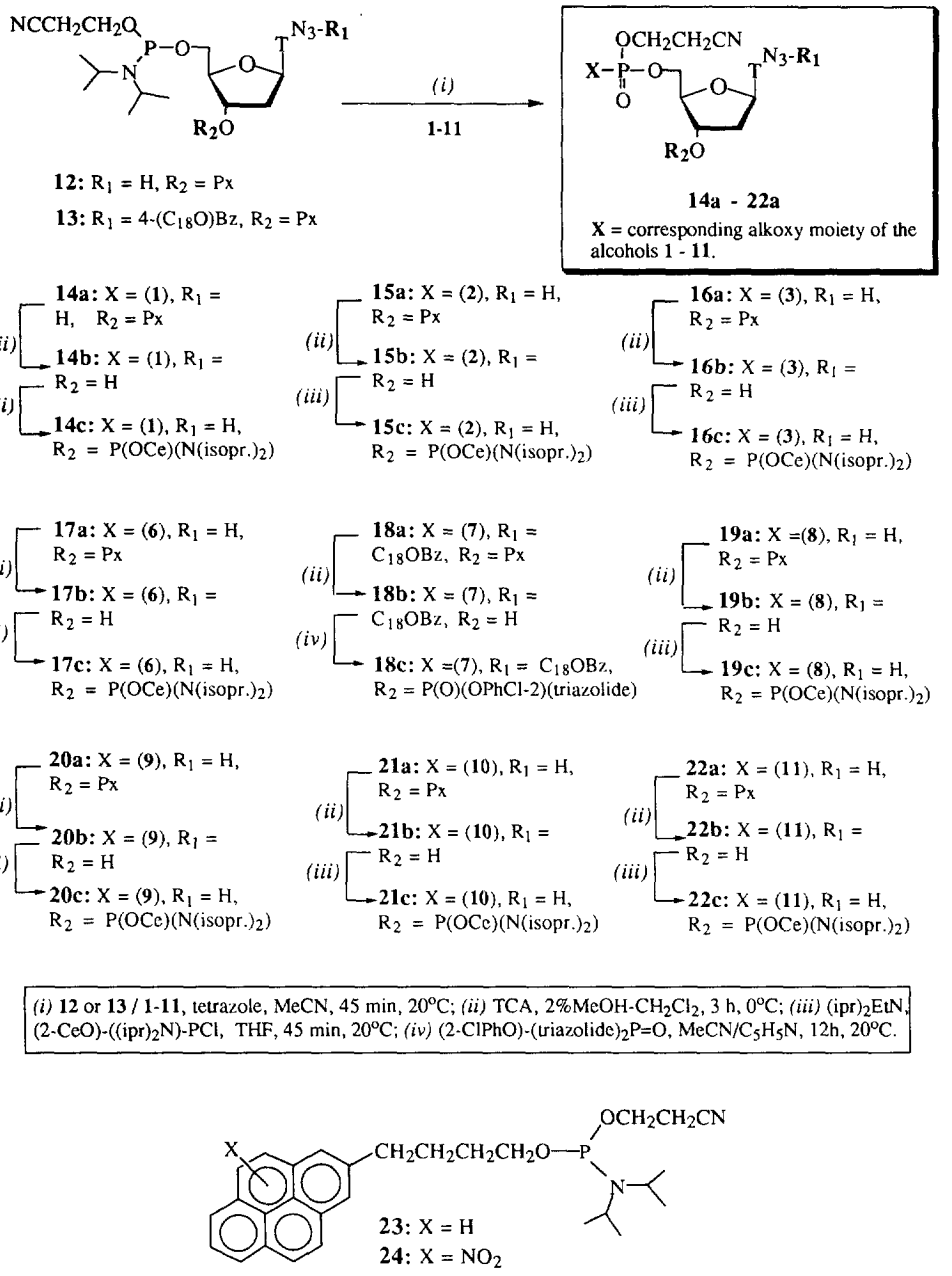

Fig. 2

(B) Thermal stabilities of the duplex formed with the 9-mer oligo probes ***29-40*** *and the targets* ***25*** *,* ***26*** *and* ***28****.*

Duplexes with 5'-tethered chromophores were generated by hybridisation of 9-mers **30-40** with target

duplexes **25** and **26** in a 1:1 ratio with 1μM of each strand in 20 mM PO_4^{3-}, 0.1M NaCl buffer at pH 7.3. The complementary nucleotide sequence within these duplexes was the same as the one that had been used in our previous investigations.[6] All the melting curves of these duplexes showed a monophasic dissociation and Table 1 shows the melting temperatures. Following comparisons are noteworthy: *(i)* When targets **25**, **26** and **28** were used, all chromophores increased the duplex T_m compared to the non-tethered duplex (ΔT_m ~+3-14° C). *(ii)* With targets **25**, **26** and **28**, the angular phenanthrene derivatives (entries# 2 & 3) gave the highest stabilisations (ΔT_m ~+11-14° C). Increasing the linker length with two methylenes (entry# 4) decreased the stabilisation (ΔT_m ~+5-8° C) (in contrast, the stabilisation of the triplex increases with increased chain length with two methylene groups. see Table 2). *(iii)* Anthracene (entry# 11) gave lower stabilisations (ΔT_m ~+5-8° C) than the angular phenanthrene (entry# 2). *(iv)* Decreasing the electron density of the phenanthrene ring system by nitration gave no (target **28**) or only marginal (targets **25**, **26**) increase of duplex stabilisation (entries# 2 & 3). *(v)* Pyrene (entry# 5) gave no (target **26**) or a small increase of (targets **25, 28**) stabilisation compared to phenanthrene with linker chains of similar length (entry# 4). *(vi)* Nitration of pyrene destabilised the duplexes (entry# 6 as compared to entry# 5). *(vii)* Phenazine (entry# 7) gave similar duplex stabilities (ΔT_m ~+10-11.5° C) to those of phenanthrene derivatives (entries# 2 & 3) in case of targets **25**, **26**, but for mismatch target **28** considerably lower. *(viii)* The 9-*N*-ethylphenazinium (entry# 8) tether, with a lower electron density than phenazine itself, gave a marginal increase of duplex stabilisation (compared with entry #7) with targets **26**, **28**, but not with **25**. *(ix)* Of the two naphthalene derivatives, the β-isomer gave a marginally higher stabilisation (ΔT_m ~6.5° C) than the α-isomer (ΔT_m ~+5-6° C) with the short targets **25**, **26**, but the stability was reversed with the mismatch target **28** (entries# 9 & 10). *(x)* Fluorene (entry# 12) proved to be the poorest stacker in these duplex systems (ΔT_m ~+3-5° C).

*(C) Thermal stabilities of the duplexes formed with the 9-mer probes **29 - 40** and the matched 20-mer oligo-DNA **27** and their comparison with those formed with the mismatched analogue **28**.*

The melting curve of **27** alone (obtained in an identical condition as described in the section C) showed a clear monophasic dissociation (ΔT_m = 37.6° C), which is a clear evidence that it is folded into some defined tertiary structure. Interestingly, when an equimolar ratio of either of the conjugates **29** - **40** and **27** was heated to 70° C, and then cooled to 15° C, we found that the above T_m was unaltered, suggesting that the thermodynamic stability of the folded **27** was much larger than any other duplex that could have been formed with any of the conjugates **29** - **40** and **27**. We can envision three possible secondary structures for **27** (Fig. 3) that would have reasonable thermodynamic stability: Duplex (**A**) with two A-A mismatch basepairs and four minor tautomer form of G-T mismatch[17a-d] (or any of the G-T basepairs adopting the wobble structure[17a]) along with twelve fully matched basepairs. G-T basepairing has been shown by crystal structure analysis[17c,d] and we can expect these to contribute to the duplex stability, although their ΔG values are somewhat more positive than normal fully matched basepairs.[17a] The second possible structure for **27** is a hairpin (**B**) (Fig. 3) with one A-A mismatch along with six fully matched basepairs in the stem part and with a six nucleotide hairpin loop, which is most probably thermodynamically more preferred over the duplex (**A**) for **27** (it is known that the hairpin structures are more stable than the corresponding duplex[18]). Duplex (**C**) could also be possible with eight fully matched basepairs in a row without any mismatch interruptions, which was ruled out by the synthesis of two 18-mers, 5'-d(TTAACATGTTTGGACAAG)-3' (T_m = 31.2° C) & 5'-d(AACATGTT TGGACAAGTT)-3' (T_m = 36.5° C), in which two thymine bases were removed from 3'- or 5'-end, respectively, of the 20-mer **27**. Since, the 18-mer, 5'-d(AACATGTTTGGACAAGTT)-3' [compared to 5'-d(TTAA

CATGTTTGGACAAG)-3'] shows the same stability as the 20-mer **27** , the two thymine bases at the 3'-end are important for the folding, suggesting that the (**A**) and (**B**) in Fig. 3 are likely secondary structures for **27**.

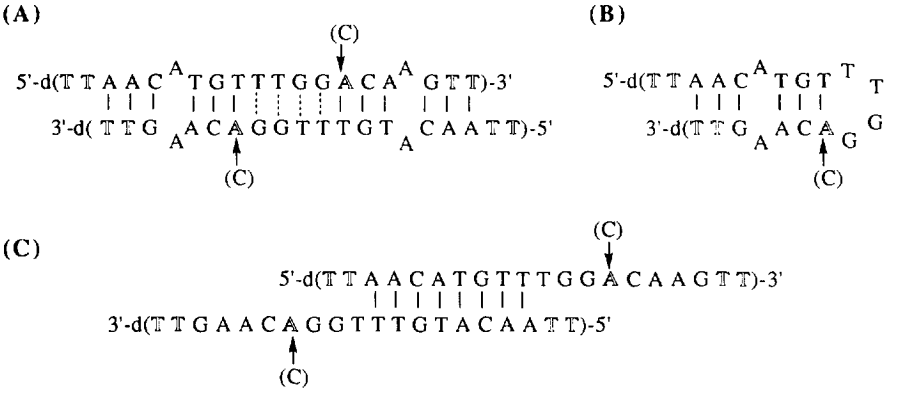

Fig. 3. Possible stable secondary structures of 20-mer target **27**.

Exchanging A for a C residue in **27** (Fig. 3) generated a mismatch 20-mer **28** with a thermal stability ~10° C lower than **27**. This made it possible for each of the oligonucleotide-conjugates **29** - **40** to compete with the mismatched 20-mer strand **28**, and form the expected complementary antisense duplexes (Table 1). This sensitivity to single-point change from A to C also suggests that **27** is most probably folded in to the secondary structures such as **A** and **B**.

Thus, this set of experiments with **27** and **28** showed the danger in only taking the primary structure of the target sequence into account when designing antisense oligomers.[19a,b] This is fully consistent with Matteucci's recent observation that "There are a few sites that are accessible, kinetically available, and those are the targets".[19a]

*(D) Thermodynamic measurements of duplexes of 5'-tethered oligos **30** - **40** with targets **25, 26, 28***

The $\Delta G°$(298K)[20] for duplexes between the targets **25**, **26**, **28** and 9-mers **30**-**36** were found around -42 ±6 kJ mol^{-1}, which were thermodynamically more stable as compared to the corresponding duplexes of **29**(blank)+**25/26** as well as **38**(β-naphthalene)+**28**, **40**(fluorene)+**28**, **40**+**26** ($\Delta G°$(298K) -34 ±6 kJ mol^{-1}). The α and β-naphthalene conjugates **37** and **38** formed duplexes with targets **26**(+**37/38**) and **28**(+**37**) with intermediary thermodynamic stability ($\Delta G°$(298K) -37 ±4 kJ mol^{-1}). No useful conclusions could be made from the above thermodynamic measurements, hence further quantification of duplex stability was discontinued.

*(E) Fluorescence measurements of duplexes of 5'-tethered oligos **30** - **40** with targets **25** - **28***

Different types of oligonucleotide tethered polycyclic aromatic chromophores are known to generate different fluorescence properties upon interaction with oligonucleotides. These properties are to some extent dependent on the nature of the nucleotides with which the chromophore interacts[21], and also in the manner in which the chromophore is tethered. The oligonucleotide-tethered anthracene has been shown to give fluorescence enhancement and blue shift of the emission maximum upon duplex formation[22] when the 2-

Table 2 : The thermal stability of triplexes & duplexes (T_m in °C) resulting from a 1:1:1 mixture of octadecamer conjugates **43-54** with the duplex: **41+ 42.***

		pH 7.3								pH 6.5				pH 6.0			
Entry#	5'-X-18-mer conjugates	Triplex				18+24 duplex				Triplex		18+24 duplex		Triplex		18+24 duplex	
		Mg^{2+}		no Mg^{2+}		Mg^{2+}		no Mg^{2+}		no Mg^{2+}		no Mg^{2+}		no Mg^{2+}		no Mg^{2+}	
		T_m	ΔT_m	T_m	ΔT_m	T_m	ΔT_m	T_m	ΔT_m	T_m	ΔT_m	T_m	ΔT_m	T_m	ΔT_m	T_m	ΔT_m
1	**43**	21.4	-	13.5	-	54.9	-	42.8	-	21.5	-	42.0	-	25.6	-	41.8	-
2	**44**	31.4	10.0	17.5	4.0	60.3	5.4	50.3	7.5	24.8	3.3	50.1	8.1	30.0	4.4	49.9	8.1
3	**45**	36.3	14.9	18.2	4.7	59.6	4.7	51.1	8.3	25.6	4.1	51.0	9.0	31.0	5.4	50.5	8.7
4	**46**	33.8	12.4	18.7	5.2	59.5	4.6	48.5	5.7	25.0	3.5	48.4	6.4	n.d.	-	47.5	5.7
5	**47**	33.2	11.8	16.0	2.5	59.6	4.7	49.8	7.0	23.9	2.4	49.5	7.5	29.5	3.9	49.1	7.3
6	**48**	n.d.	-	17.9	4.4	59.6	4.7	49.4	6.6	25.9	4.4	49.7	7.7	31.0	5.4	49.2	7.4
7	**49**	32.0	10.6	17.4	3.9	57.5	2.6	46.6	3.8	24.3	2.8	45.8	3.8	30.3	4.7	45.1	3.3
8	**50**	n.d.	-	n.d.	-	57.4	3.5	46.9	4.1	n.d.	-	46.4	4.4	n.d.	-	45.1	3.3
9	**51**	19.9	-1.5	12.3	-1.2	57.9	3.0	47.0	4.2	19.6	-1.9	46.1	4.1	22.5	-3.1	46.0	4.2
10	**52**	23.0	1.6	14.3	0.8	59.1	4.2	48.7	5.9	21.4	-0.1	47.6	5.6	25.6	0.0	47.0	5.2
11	**53**	22.8	1.4	14.0	0.5	57.2	2.3	46.8	4.0	19.2	-2.3	46.6	4.6	26.9	1.3	45.8	4.0
12	**54**	19.5	-1.9	13.0	-0.5	57.2	2.3	46.1	3.3	21.8	0.3	46.3	4.3	24.9	-0.7	45.7	3.9

n.d. implies could not be determined.

* The protocol for measuring the T_m of the duplexes and triplexes is reported in the experimentals.

anthracenylmethyl moiety tethered to a uridine 2'-hydroxyl group was incorporated into the oligomer. But when 9-anthracenylmethyl was tethered to the 2-amino of guanosine, a quenching of fluorescence (no shift in emission maximum) was observed.[23] The oligonucleotide tethered pyrene has shown similar ambiguity. When the 1-pyrenylmethyl moiety was tethered to a uridine 2'-hydroxyl group and this block incorporated into an oligomer, on hybridisation to a RNA target sequence a large enhancement of fluorescence and a blue shift was observed.[24] But when 4-(pyren-1-yl)butyric acid was tethered through an amino linker to the C4 of thymidine, a quenching of fluorescence and red shifts were observed upon duplex formation.[25a,b] The same quenching was also observed when the pyren-1-yl moiety was directly connected to the C1' in 2-deoxyribose and incorporated into an oligomer.[26] The oligonucleotide-tethered heteroaromatic hydrocarbons such as substituted acridine derivatives have been shown to give fluorescence enhancements and blue shifts of emission maximum upon interaction with complementary oligonucleotides.[27a-c] The same has been shown for ethidium conjugates[28] and conjugates of Hoechst derivatives.[29a,b] The acridine chromophore has however shown a fluorescence quenching when an acridine tethered oligonucleotide was hybridised to a duplex to form a triplex.[30] Large changes (ΔF) in fluorescence intensity (FI) have been correlated to strong intercalation of the chromophore between nucleobases[27b,c] or deep embedment into the duplex minor groove,[29a,b] while small or moderate changes have been attributed to binding (stacking) of the chromophore exterior to the stacked nucleobases of the opposite strand in duplexes or to their orientation in the minor groove.[23]

In this work, fluorescence measurements were carried out for each chromophore **1** - **11** and for their oligo-tethered forms **30** - **40** at 20-23° C in 20 mM PO_4^{3-}, 1M NaCl at pH 7.3, and the results were compared. This comparison was based on the complete set of derivatives of the chromophore such as **A** [free hydroxy alkylated chromophore] → **B** [5'-chromophore-tethered thymidine] → **C** [5'-chromophore-tethered single 9-mer strand] → **D** [duplex of 5'-chromophore-tethered single 9-mer strand with **25-28** targets]. This allowed us to evaluate the mode of interaction between the 5'-tethered-chromophores and the oligonucleotides. For each chromophore, the FI was measured for each state in the series **A** → **B** → **C** → **D**, and ΔF values were calculated[29a] using the ΔF value for all chromophores in state **C** as 1.0. In case of multiple fluorescence peaks, the highest peak was used for ΔF calculations.

The largest changes in ΔF were observed when comparing the states **A** with those of **B** for all chromophores [compare ΔF for state **A** for **1** (2.7), **2** (5.6), **3** (15.1), **4** (178.1), **5** (2.6), **6** (0.1), **7** (0.3), **8** (41.4), **9** (100.0), **10** (21.8) and **11** (3.4) with those of the corresponding ΔF values for state **B** for **1** (1.1), **2** (5.1), **3** (1.3), **4** (14.1), **5** (1.1), **6** (0.6), **7** (1.0), **8** (2.8), **9** (1.6), **10** (2.6), **11** (6.0)]. For chromophores **1** - **5** and **8** - **10**, a fluorescence quenching was observed from state **A** → **B**, thereby suggesting a stacking interaction between the chromophore and the thymine base at the monomer level. In case of **2** and **5**, there seem to be a correlation between reduction of the electron density in the ring systems by nitration and reduction in the change in fluorescence intensity when comparing the state **A** with **B**. Both the phenazine derivatives (**6** & **7**) as well as the fluorene chromophore (**11**) experienced a considerable increase in ΔF when going from state **A** → **B**.

When comparing the state **B** with **C**, small to large quenching ($\Delta\Delta F$ -0.1 to -14.1) were observed, except for the phenazine derivatives (**6** & **7**) ($\Delta\Delta F$ +0.4 and 0.0 respectively). The nitropyrene chromophore **5** however showed no change in the fluorescence intensity ($\Delta\Delta F$ 0.0).

A comparison of the single strand state **C** with the double strand state **D** (with short targets such as 10-mer **25** and 11-mer **26**) practically showed no changes in ΔF ($\Delta\Delta F$ was within the range +0.1 and -0.3), suggesting only minute changes in the microenvironment of the chromophore. However, two notable

exceptions were observed: (i) The phenazinium chromophore **7** when complexed to target **25** or **26** experienced a 5-fold decrease of ΔF, whereas (ii) the α-naphthalene **8** experienced an increase in ΔF (ΔΔF +0.6) with target **25** along with the appearance of a large new signal (ΔF +11.8). In these two cases, some pronounced changes in the microenvironment of the chromophore are likely. With longer targets such as matched 20-mer **27** and the mismatched 20-mer **28**, very little changes in ΔF was observed for chromophores **3, 7, 8, 9, 10, 11** (ΔΔF was within the range of +0.3 and -0.3), but for chromophores **1, 2, 4, 5** an unambiguous increase in ΔF was observed (ΔΔF was in the range +0.3 and +7.3), which seem to imply a weakening of interaction between these chromophores and the neighbouring nucleotide(s) of the targets **27** and **28** compared to **25** and **26**.

We also examined the Stoke's shifts when comparing the different states from **A** → **B** → **C** → **D**. The excitation wavelengths are given in the experimental part. The emission wave lengths of the main peak of the 5'-chromophore-tethered thymidine blocks were as follows: **1** (378 nm, 3 peaks), **2** (491 nm), **3** (409 nm, 2 peaks), **4** (377 nm, 3 peaks), **5** (399 nm), **6** (630 nm), **7** (633 nm), **8** (367 nm, 2 peaks) and **9** (374 nm, 2 peaks), **10** (422 nm, 3 peaks), **11** (346 nm). In cases of chromophores **1, 3, 4, 5, 9, 11**, neither blue nor red shifts connected to the main peak was observed throughout the whole series: **A** → **B** → **C** → **D**. Blue shifts were observed in following transitions: (i) Nitro phenanthrene chromophore (**2**): [**A** → **B** ($\Delta Abs \approx 17$ nm), **B** → **C** ($\Delta Abs \approx 46$ nm)]. (ii) Phenazine chromophore (**6**): [(**A** → **B** ($\Delta Abs \approx 4$ nm), **B** → **C** ($\Delta Abs \approx 14$ nm)]; **D** (targets **25** & **26**) → **D** (targets **27** & **28**) ($\Delta Abs \approx 15$ nm)]. (iii) Phenazinium chromophore (**7**): [**A** → **B** ($\Delta Abs \approx 14$ nm), **B** → **C** ($\Delta Abs \approx 15$ nm)]. Red shifts were observed in the following cases: (i) Anthracene[23] chromophore (**10**): (**A** → **B** (ΔAbs (3 peaks) ≈ 4, 4, 4 nm), **B** → **C** ($\Delta Abs \approx 3, 2, 6$ nm). (ii) α-isomer of naphthalene (**8**): [(**A** → **B** ($\Delta Abs \approx 9$ nm)].

No shifts in the fluorescence emission maxima were observed when comparing state **C** (single strand) with **D** (double strand). All the observed shifts took place when moving from state **A** (free chromophore) → **B** (monomer) → **C** (single strand), except in the case of the phenazine chromophore (**6**), where a considerable blue shift took place in the double strand state with the longer target oligomers **27, 28**, but no such shift was found with the short target oligomers such as **25** and **26**.

It is noteworthy that there are no unambiguous correlation between T_ms presented in Table 1 and the fluorescence data presented above. This is consistent with earlier results,[27c] where it was argued that the ΔF of the chromophore not necessarily reflects the thermal stability of the DNA structure, but rather the microenvironment around the chromophore.

Our fluorescence data cannot be clearly correlated to the mode of chromophore - nucleotide interaction that takes place in the single strand state vis-a-vis double strand (**C** → **D**), although the weak changes in ΔF for chromophores **1 - 6, 8 - 11** suggest stacking of the chromophores with nucleobases of the opposite strand in the duplexes, consistent with our NMR studies[6] (see below).

The fluorescence behaviour of 9-*N*-ethylphenazinium chromophore **7**, as its 9-mer conjugate **36** hybridised to targets **25** and **26**, is of special interest in regard to the elaboration of the mode of chromophore - nucleotide interaction. Detailed NMR studies have earlier been carried out in this laboratory on the analogous 5'-tethered *N*-(2-hydroxyethyl)phenazinium duplex[6] shown in Fig. 4. These NMR studies unambiguously showed that the 5'-tethered *N*-(2-hydroxyethyl)phenazinium chromophore was intercalated between two nucleobases of the opposite strand. We argued that a direct comparison and subsequent correlation of the fluorescence characteristics of this duplex with its observed NMR structure will shed some light on the interpretation of the above fluorescence data. With this in mind, we measured the fluorescence of the 5'-

phenazinium tethered cytidine block, 5'-phenazinium tethered 7-mer single strand and its duplex with the complementary 8-mer. We found the same extent of fluorescence quenching ($\Delta\Delta F$ = -0.8) from the single to the double strand as in the case of 9-mer single-stranded conjugate **36** and its duplexes with **25** and **26**. From this comparison between NMR structure and the fluorescence data, we can safely conclude that the 5-fold fluorescence quenching observed between single and double strand (*i.e.* between **36** and **36+25** or **36+26**) is due to the intercalation of the 9-*N*-ethylphenazinium chromophore between C and A nucleotide residues in the opposite strand as in **26**.

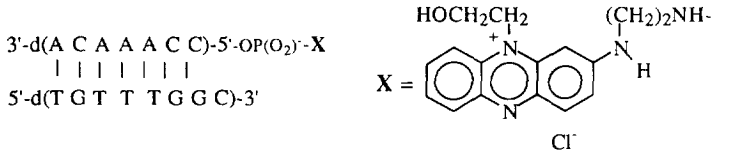

Fig. 4. The 5'-Phenazinium-7-mer + 8-mer duplex earlier studied by NMR.[6]

*(F) Thermal stabilities of triplexes formed with the 5'-chromophore-tethered 18-mer probes **44-54** and the duplex target [41+42]*

Triplexes with chromophores **1 - 11** tethered to the 5'-end of the third strand were generated by hybridisation of 18-mers **43-54** with 24-mer duplex **41:42**[5e] in a 1:1:1 ratio with 1μM of each strand in buffer A [20 mM PO_4^{3-}, 0.1M NaCl at pH 7.3, 6.5 and 6.0], and in buffer B [25 mM TrisHCl, 0.1M NaCl, 20mM $MgCl_2$ at pH 7.3]. The third strand pyrimidine-rich T-C sequences **43-54** were expected to Hoogsteen basepair in a parallel orientation[1c,5e] to the complementary purine-rich G-A sequence in the target duplex **41:42**. Furthermore, the stability of these triplexes was expected to be pH-dependent because it is only protonated cytosine that can form a stable CH$^+$*G:C triplet.[1c, 5e]

All melting curves obtained from a solution of **41** & **42** with each of the oligonucleotide-conjugates **43** - **54** showed a triphasic dissociation behaviour. In buffer A in the pH range 6.0-7.3, the transition observed in the temperature range 12-32° C corresponded to dissociation of the third strand, the transition observed in the temperature range 42-51° C corresponded to the dissociation of the mismatch duplex between the 18-mer and the GA-rich 24-mer, while the transition observed in the temperature range 61-63° C corresponded to the dissociation of the **41:42** 24-mer duplex. In buffer B (with Mg^{2+}), the same triphasic dissociation behaviour was observed with the corresponding temperature ranges of 20-36°, 55-60° and 69-69.5°C.

Table 2 shows the melting temperatures of these triplexes and duplexes in the pH range 6.0-7.3. Following comparisons are noteworthy: (i) Triplex formation, as well as 18+24-mer duplex formation took place with all 18-mers including the blank 18-mer **43** at all pH, except for **50** for which no triplex formation was detected at any pH with or without Mg^{2+}. Also for **48** no triplex was detected at pH 7.3 with Mg^{2+}. Expectedly, the triplexes showed increased stability towards lower pH, while the duplexes showed decreased stability. (ii) The 5'-α- and β-naphthalene- (**51**, **52**), the 5'-fluorene- (**54**) and the 5'-anthracene- (**53**) tethered 18-mers gave no triplex stabilisation at any pH, but induced 18+24-mer stabilisation (ΔT_m ~+3-6° C). (iii) The angular phenanthrene tether (entry# 2) was a more efficient triplex (ΔT_m ~+3.5-4.5° C) and duplex (ΔT_m ~+7.5-8° C) stabilising agent than the linear anthracene tether (entry# 11) ($\Delta T_{m,\,triplex}$ ~-2.5-+0.5° C, $\Delta T_{m,\,duplex}$~+1.5-4° C) at all pH. (iv) Decreasing the electron density of the phenanthrene ring system by nitration made the triplex more stable (entries# 2 & 3) (ΔT_m ~+4-5.5° C) at all pH. The same holds true even when the pyrene

chromophore (entry# 5, ΔT_m ~+2.5-4° C) was converted to the nitropyrene chromophore (entry# 6, ΔT_m ~+4.5-5.5° C). The corresponding 18+24-mer duplexes also showed the same trend at all pH. However, in Mg^{2+}-buffer at pH 7.3 no triplex was detected for the nitropyrene conjugate **48** (entry #6). (v) Phenazine (entry# 7) generated comparable triplex stabilities (ΔT_m ~+4-5° C) to that of phenanthrene (entries# 2 & 3) at all pH. However, the phenazine-tethered 18+24-mer duplex was considerably less stable. (vi) The 9-*N*-ethylphenazinium tether, (entry# 8) generated no detectable triplex at any pH, but gave 18+24-mer duplex with stabilities (ΔT_m ~+4-5° C) similar to the corresponding phenazine-tethered duplex. (vii) Increasing the linker length with two methylenes on phenanthrene (entries# 4) increased the triplex stability (ΔT_m ~+5.2° C; 12.4° C (Mg^{2+})) at pH 7.3 compared to the shorter linker (entry# 2). Note that the 18+24-mer duplex showed the opposite trend (see Table 1). Hence, for triplex formation, a longer linker is more beneficial for the stabilisation than in case of duplex formation.

(G) Fluorescence measurements of triplex mixtures.

Triplexes with 5'-chromophore-tethered 18-mers **44**, **45**, **47**, **48** and **49** were selected for fluorescence measurements because they were found to induce greater stabilisation in the duplex study. The ΔF values were calculated[29] from the FI of state **B** (18+24+24 triplex / 18+24 duplex mixtures of 5'-chromophore-tethered 18-mers mixed with the 24-mers **41** and **42**) and state **A** (5'-chromophore-tethered 18-mer single strand). The measurements of solutions of **A** and **B** were carried out in 20 mM PO_4^{3-}, 1.0M NaCl at pH 6.0. From these measurements following conclusions can be made: (i) A 30-fold increase in ΔF at the emission wavelength 380 nm was observed when the pyrene conjugate **47** was hybridised to **41**+**42**, indicating a major change in the microenvironment of the pyrene chromophore. No change occurred for the nitropyrene conjugate **48**. In either case no shift in emission maxima occurred. (ii) When phenanthrene conjugate **44** was mixed with **41**+**42**, the ΔF increased by 1.3-fold at the emission wavelength of 347 nm, and by 2.7-fold at the emission wavelength 382 nm. For nitro phenanthrene conjugate **45**, the ΔF decreased by 1.2-fold at the emission wavelength of 461 nm for **A** compared to state **B** which had an emission maximum at 468 nm (*i.e* a red shift of ~7 nm from state **A**→**B**); the ΔF for **45** also decreased by 2.5-fold at the emission wavelength of 544 nm from state **A** to **B** with no Stoke shift. (iii) When the phenazine conjugate **49** was mixed with **41**+**42**, a 1.3-fold increase in ΔF was found at the emission wavelength of 616 nm for state **A** to **B** (blue shift of~11 nm).

CONCLUSION

In this work, eleven different planar hydroxy alkylated polyarenes **1**-**11** were synthesised, and used for the preparation of 5'-chromophore-tethered oligonucleotides **30**-**40**, **44**-**54** for testing their abilities to form stable duplexes and triplexes. Our main objectives were as follows: (i) Is there any correlation between physico-chemical properties of the chromophore (such as geometry, bulk, electronic properties, polarisability, hydrophobicity) and the duplex or triplex stability? (ii) Can we influence the duplex stabilities by changing the stacking site of the 5'-tethered-chromophore with different target duplexes? (iii) How does the folding of the target oligonucleotides influence the binding properties of a complementary antisense strand? (iv) And, finally, determine the mode of interaction between the chromophore and nucleotides upon duplex or triplex formation by using fluorescence and NMR data.[6]

We used blank 9-mer **29** and the 5'-chromophore-tethered 9-mers **30** - **40** for formation of duplexes with

four different targets: (1) The 10-mer DNA **25**, in which the chromophore moiety in **30** - **40** is "dangling" at one of the terminus of the duplex. (2) The 11-mer DNA **26**, in which the stacking position of the chromophore in **30** - **40** is at the penultimate nucleotide from the 3'-terminus of the opposite strand. (3) The 20-mer fully matched DNA **27**, in which the stacking position is in the interior of the duplex, and (4) the 20-mer mismatched DNA **28**, with the mismatch basepair being placed at the stacking site of the chromophore. The sequence of **27** and **28** were chosen such that they also should be able to intramolecularly fold into organised secondary structures (Fig. 3), and then examine if a complementary 5'-chromophore-tethered DNA sequence could competitively bind to this self-assembled target. In addition, we used the blank 18-mer **43** and its 5'-chromophore-tethered derivatives **44** - **54** for formation of the triplexes with the 24-mer duplex targets **41+42** , in which the 5'-tethered-chromophore is expected to stereochemically orient itself inside the triplex.

We used T_m and fluorescence measurements as the main tools to study the physico-chemical properties of the chromophore, which led us to the following conclusions: (i) four atoms between the chromophore ring system and the phosphorous of the 5'-phosphate (chromophore-X-CH_2CH_2OP) gave higher duplex stability[12a] than the linker containing 6 atoms (entries 2 & 4 in Table 1); however the reverse was observed for the triplex stability (entries 2 & 4 in Table 2). (ii) Increasing the bulk and the hydrophobicity of the chromophore produces some duplex stabilisation, as is exemplified by pyrene (entry 5, Table 1) and phenanthrene (entry 4, Table 1) of similar linker lengths. However, in case of triplex formation this situation was reversed (entries 4 & 5, Tables 1 & 2). Decreasing the size of the polycyclic aromatic ring system further decreases the duplex/triplex stability, as exemplified by the β/α-naphthalenes (entries 9 & 10, Tables 1 & 2). (iii) The geometry of the chromophore had some bearing on the duplex/triplex stability, as exemplified by the angular phenanthrene (entry 1, Tables 1&2) in comparison with the linear anthracene (entry 11, Tables 1 & 2), thereby suggesting that the angular phenanthrene is a more efficient stacker. (iv) Decreasing the electron density of the phenanthrene ring system by nitration produced higher duplex/triplex stabilisations (entries 2 & 3, Tables 1 & 2), indicating a more efficient π-π electron interaction between the 5'-tethered-chromophore and the nucleobases involved, possibly due to less π-π electron repulsion or a more efficient donor-acceptor charge transfer.[7] Similarly, decreasing the electron density of the pyrene ring system by nitration produced higher triplex stabilisation (entries 5 & 6, Table 2). However, it produced practically no stabilisation of the 18+24-mer duplex, and a destabilisation of duplexes between 9-mers and targets **25**, **26**, **27**, **28** (entries 5 & 6, Table 1), thereby indicating different modes of π-π electron interaction for duplex and triplex formation in case of pyrene. (v) By changing the electronic properties of anthracene by exchanging the 9,10-carbons with two nitrogen atoms to generate phenazine produced higher triplex stability (entries 7 & 11, Table 2). With Mg^{2+}, this stabilisation effect was considerably higher, indicating some additional chelating effect involving the lone pairs of the phenazine nitrogens, Mg^{2+} and oligonucleotide strand. However, in regard to 18+24-mer duplex, no stabilisation occurred. On the other hand, duplex stabilisation was observed when the 9-mer strands were hybridised with targets **25** and **26**, but not with **27** and **28** (entries 7 & 11, Table 1). (vi) Decreasing the electron density of the phenazine ring system by 9-*N*-ethylation produced only a weak stabilisation in duplexes of 9-mer and target **26** and **28** (entries 7 & 8, Table 1) and for the 18+24-mers (pH7.3 & 6.5) (entries 7 & 8, Table 2). No triplex formation was observed with the phenazinium-tethered conjugate **36**.

The T_m measurements showed practically no difference in duplex stability between targets **25** (10-mer) and **26** (11-mer), when they were charged with the 9-mer oligos **29**-**40**. With mismatched 20-mer target **28**,

the duplex stabilities dropped by 2-9° C compared to **25** and **26**. No conclusion on duplex stability could be made from mixing **29-40** with matched 20-mer target **27**, because the latter has a profound thermodynamically stable tertiary structure(s) (Fig. 3). However, we were able to weaken the thermal stability of the tertiary structure of **27** by exchanging one matched basepair with one mismatched basepair, which generated target **28**. This made it possible to generate duplexes with each of **29-40** and **28**. This experiment showed that the tertiary structures of the target oligonucleotide should be considered very carefully when choosing an antisense target.

Fluorescence studies on single strand to double strand transition suggest weak interaction between the 5'-tethered-chromophore of **30-40** and the nucleotides in targets **25-28**. The exception was the 5-fold quenching of fluorescence observed with the transition from the single strand of 5'-9-*N*-ethylphenazinium conjugate **36** to its duplex with the 11-mer target **26**. The reason for this fluorescence quenching was explained basing upon the comparison of the known NMR solution structure of the analogous 5'-tethered *N*-(2-hydroxyethyl)phenazinium duplex[6] (Fig. 4), in which we have earlier unambiguously shown that the phenazinium ion was indeed intercalated between nucleotide residues in the opposite strand. Since this duplex (Fig. 4) underwent the same fluorescence quenching from the transition of the single to the double strand in a similar way as found for the transition of the single strand **36** to its duplex with **26** (*i.e.* **36+26** duplex), we concluded that the observed fluorescence quenching found in **36+26** duplex is owing to the intercalated state of the chromophore **7**.

Comparison of the fluorescence intensities of the single stranded 5'-chromophore-tethered 18-mers **44**, **45**, **47**, **48**, **49** with the corresponding 18+24+24-mer triplex and 18+24-mer duplex mixtures, shows no or only moderate changes in ΔF, which is most probably indicative of weak exterior binding of the chromophore to the nucleobases. One exception was the pyrene conjugate **47**, which gave a large fluorescence enhancement, indicative of some major change in the microenvironment of the pyrene chromophore either during duplex or triplex formation or both.

In summary, our conclusions are as follows: (i) The changes in the bulk and electron density of the tethered-chromophore influences the thermal stability of the DNA duplex/triplex structures. (ii) Antisense hybridisation is very sensitive to the tertiary structures of the target oligonucleotide sequence. This means that the T_m data produced on a short target DNA as that of the size of the antisense oligo is of little value for extrapolation on a larger target sequence. (iii) The fluorescence properties of the chromophore-tethered DNA structures reflect the microenvironment of the chromophore rather than the thermal stability of the structure. (iv) When fluorescence properties are to be correlated to the mode of chromophore - nucleobase interaction during formation of a chromophore-tethered DNA secondary / tertiary structure, it was proven beneficial to interpret the fluorescence data basing on the NMR structural analysis, as shown in case of conjugate **36**.

EXPERIMENTAL

^{1}H-NMR spectra were recorded in δ scale on a Jeol JNM-GX 270 spectrometer at 270 MHz, using TMS as an internal standard. ^{31}P-NMR spectra were recorded at 36 MHz in the same solvent using 85 % phosphoric acid as external standard. ^{13}C-NMR spectra were recorded at 69 MHz (270 MHz ^{1}H-NMR) in the same solvent using the solvent resonance as the internal standard. TLC was carried out using pre-coated silica gel F_{254} plates in the following dichloromethane-methanol mixtures: (A) 98: 2 (v/v), (B) 95:5 (v/v), (C) 90:10 (v/v). Dry pyridine was obtained by distillation over 4-toluenesulphonyl chloride. Acetonitrile and dichloromethane were distilled from P_2O_5 under argon. Dimethylformamide was distilled over CaH_2. 4-(1-octadecyloxy)benzoyl

chloride (bp. ~240° C / 0.15 mmHg) was prepared by *O*-alkylation of the sodium salt of ethyl 4-hydroxybenzoate with 1-bromooctadecane,[31] followed by alkaline ester hydrolysis and chlorination with thionyl chloride. All reactions in this work were carried out at room temperature (20-23° C) unless otherwise stated. The column chromatographic separations of all the protected intermediates were carried out using Merck G 60 silica gel. A Gilson equipment with Pump Model 303, Manometric Module Model 802C and Dynamic Mixer 811B connected to a Dynamax computer program for gradient control was used for semi-preparative RP-HPLC separations on Spherisorb 5ODS2. Melting measurements were carried out using a PC-computer interfaced Perkin Elmer UV/VIS spectrophotometer Lambda 40 with PTP-6 peltier temperature controller. The thermodynamic calculations were carried out using Profit computer calculation program. Fluorescence measurements were carried out using an Aminco SPF-500 Corrected Spectra Spectrofluorometer with a Xenon lamp power supply.

*9-(2-hydroxyethoxy)phenanthrene (**1**).*

9-hydroxyphenanthrene (777 mg, 4 mmol) was dissolved in dry dimethylformamide (2 ml) followed by addition of potassium *tert*-butoxide (403 mg, 4.2 mmol). Then 1-*O*-(4-methoxytrityl)-2-chloroethane (706 mg, 2 mmol) was added and the dark suspension was heated to 75 °C and stirred for 4 h. The reaction mixture was worked up by aqueous 0.1M NaOH - dichloromethane extraction and the obtained organic residue was silica gel column chromatographed (Hexane:CH_2Cl_2, 70:30 v/v) to give the intermediary *9-(2-O-(4-methoxytrityl)ethoxy) phenanthrene* . This material was dissolved in 80% acetic acid (8 ml) / dioxane (2 ml) and stirred for 1 h at 50°C. After removal of solvent by rotary evaporator the residue was silica gel column chromatographed (Hexane:CH_2Cl_2:EtOH, 70:30:0 to 0:98:2 v/v/v) to give the title compound **1** (257 mg, 54%). R_f: 0.50 (A);^{1}H-NMR ($CDCl_3$): 8.67-8.56 (m, 2H) arom.; 8.37 (d, 1H) arom.; 7.77-7.49 (m, 5H) arom.; 6.99 (s, 1H) H10; 4.36 (t, J = 4.40Hz, 2H) -O*C*H_2CH_2OH; 4.15 (t, 2H) -OCH$_2$*C*H_2OH; 2.11 (br, 1H) OH; ^{13}C-NMR ($CDCl_3$): 127.4, 127.1, 126.8, 126.3, 124.4, 122.5, 122.4, 122.2, 103.0 (arom.); 69.3 (C1); 61.5 (C2).

*9-(4-hydroxybutoxy)phenanthrene (**3**).*

Procedure analogously as for **1**, starting from 9-hydroxyphenanthrene (777 mg, 4 mmol), but using 1-*O*-(4-methoxytrityl)-4-chlorobutane (1.02 g, 2.67 mmol) and heating for 12 h. Silica gel column chromatography of the intermediary *1-(2-O-(4-methoxytrityl)butoxy)naphthalene* (Hexane:CH_2Cl_2, 70:30 v/v/v). Silica gel column chromatography of title compound **3** (0-2%EtOH/CH_2Cl_2, 240 mg, 34%). R_f: 0.55 (A); ^{1}H-NMR ($CDCl_3$): 8.64 (d, 1H) arom.; 8.58 (d, 1H) arom.; 8.37 (d, 1H) arom.; 7.78-7.45 (m, 5H) arom.; 6.98 (s, 1H) H10; 4.29 (t, 2H) 1-*C*H_2; 3.81 (m, 2H) 4-*C*H_2; 2.09 (m, 2H) 2-*C*H_2; 1.90 (m, 2H) 3-*C*H_2; 1.56 (s, 1H) OH. ^{13}C-NMR ($CDCl_3$): 127.2, 127.0, 126.8, 126.3, 124.1, 122.3, 102.6 (arom.); 67.6 (C1); 62.6 (C4); 29.6 (C2); 25.7 (C3).

*2-(N-(2-hydroxyethyl)-N-methyl)aminophenazine (**6**).*

Phenazine (1.8 g, 10 mmol) was dissolved in distilled *o*-nitrotoluene (10 ml) at 115°C, to which dimethylsulphate (2.84 ml, 30 mmol) was added and the resulting yellow-brown solution was stirred for 5 min. The solution was cooled in a cold water bath and diethyl ether (30-40 ml) was added. The dark greenish crystals were filtered and washed with diethyl ether. The crude *N*-methyl phenazinium methylsulphate[13] (2.69 g (>80%)) contained a minor amount of unreacted phenazine. The crude material (1.27 g) was dissolved in methanol (6 ml) and 2-(*N*-methylamino)ethanol was added to the yellow-green solution, which immediately turned dark-violet. This solution was stirred for 1h and then the methanol was evaporated *in vacuo*. The residue was triturated with diethyl ether (3 x 20 ml), which was decanted. The residual gum was then dissolved in concentrated ammonia (150 ml) and the dark-violet solution was stirred for 24h. The resulting red solution was evaporated *in vacuo* and the residue subjected to silica gel chromatography (1%-6%EtOH / CH_2Cl_2) to give **6** (300 mg, 28%). R_f: 0.30 (A); ^{1}H-NMR ($CDCl_3$): 8.13-8.03 (m, 2H) arom.; 7.91 (d, 1H) arom.; 7.76-7.49(m, 3H) arom.; 6.95(d, J = 2.7Hz) H1; 3.96 (t, J = 5.4Hz, 2H) -*C*H_2OH; 3.69 (t, 2H) -N*C*H_2CH$_2$OH; 3.11 (s, 3H) -N*C*H_3; 2.36 (br, 1H) OH; ^{13}C-NMR ($CDCl_3$): 141.0, 130.1, 129.34, 128.23, 127.51, 122.9, 102.5 (arom.); 60.1 (C2); 54.6 (C1), 39.2 (N<u>C</u>H$_3$).

*2-[(N-(2-hydroxyethyl)-N-methyl)amino]-9-ethylphenazinium ethylsulphate (**7**).*

Phenazine (900 mg, 5 mmol) was dissolved in distilled *o*-nitrotoluene (5 ml) at 140°C, then diethylsulphate (1.96 ml, 15 mmol) was added and the resulting yellow solution was stirred for 2h at 140°C. The solution was cooled in a cold water bath and diethyl ether (20-30 ml) was added. The dark green-brownish crystals were filtered and washed with diethyl ether. The crude *N*-ethyl phenazinium ethylsulphate[12b] (1.59 g (>80%)) contained a small amount of unreacted phenazine (5-10%). The crude material (1.37 g) was dissolved in methanol (6 ml) and 2-(*N*-methylamino)ethanol was added to the green-brown solution, which immediately

turned dark-violet. This solution was stirred for 1h and then the methanol was evaporated *in vacuo*. The residue was triturated with diethyl ether (3 x 10 ml), which was decanted. The residue was then subjected to silica gel chromatography (2-15% EtOH / CH_2Cl_2) to give **7** (709 mg, 44%). R_f: 0.15 (C); ^{1}H-NMR ($CDCl_3$): 8.32(m, 2H) arom.; 8.20-8.04 (m, 2H) arom.; 7.90(d, d 1H) arom.; 7.14, 6.85 (2 x br, 1H) H1; 5.06 (m, 2H) 9-CH_2CH$_3$; 4.93 (s, 3H) NCH_3; 4.17-4.00 (m, 6H) -NCH_2CH_2OH & CH_2 of ethylsulphate; 1.73 (t, J = 7.3Hz, 3H) 9-CH_2CH_3; 1.36 (t, J = 7.1Hz, 3H) CH_3 of ethylsulphate; ^{13}C-NMR ($CDCl_3$): 159.6, 146.3, 140.5, 137.3, 135.6, 133.4, 132.7, 128.9, 126.5, 117.5, 92.1 (arom.); 65.2 (CH_2 of ethylsulphate); 61.1 (C2); 57.1 (C1); 45.0 (9-$\underline{C}H_2CH_3$); 41.5 (N$\underline{C}H_3$); 15.7 (CH_3 of ethylsulphate); 12.5 ((9-$CH_2\underline{C}H_3$).

1-(2-hydroxyethoxy)naphthalene (8).

Starting from 1-naphtol (288 mg, 2 mmol), the procedure was analogous as that for **1**. Silica gel column chromatography of the intermediary *1-(2-O-(4-methoxytrityl)ethoxy)naphthalene* (Hexane:CH_2Cl_2, 70:30 v/v/v). Silica gel column chromatography of title compound **8** (Hexane:CH_2Cl_2, 70:30 to 0:100 v/v, 226 mg, 60%). R_f: 0.40 (A); ^{1}H-NMR ($CDCl_3$): 8.25 (m, 1H) arom.; 7.78 (m, 1H) arom.; 7.47-7.31 (m, 4H) arom.; 6.77 (d, 1H) H2; 4.20 (t, J = 4.4Hz, 2H) -OCH_2CH$_2$OH; 4.05 (t, 2H) -OCH$_2$$CH_2$OH; 2.34 (br, 1H) OH; ^{13}C-NMR ($CDCl_3$): 134.4, 127.4, 126.3, 125.6, 125.1, 121.6, 120.6, 104.9 (arom.); 69.4 (C1); 61.4 (C2).

2-(2-hydroxyethoxy)naphthalene (9).

Starting from 2-naphtol (576 mg, 4 mmol), the procedure was analogous as that for **1**. Silica gel column chromatography of the intermediary *1-(2-O-(4-methoxytrityl)ethoxy)naphthalene* (Hexane:CH_2Cl_2, 70:30 v/v/v). Silica gel column chromatography of title compound **9** (Hexane:CH_2Cl_2, 70:30 to 0:100 v/v, 271 mg, 72%). R_f: 0.40 (A); ^{1}H-NMR ($CDCl_3$): 7.73 (m, 3H) arom.; 7.47-7.18 (m, 4H) arom.; 4.20 (t, J = 4.0Hz, 2H) -OCH_2CH$_2$OH; 4.02 (t, 2H) -OCH$_2$$CH_2$OH; 2.12 (br, 1H) OH; ^{13}C-NMR ($CDCl_3$): 134.4, 129.4, 127.5, 126.7, 126.3, 122.7, 118.6, 106.8 (arom.); 69.1 (C1); 61.4 (C2).

9-(N-(2-hydroxyethyl)-N-methyl)aminomethyl anthracene(10).

9-hydroxymethylanthracene (1.2 g, 5.77 mmol) was dissolved in dry dioxane (9 ml). Thionyl chloride (525 µl, 5.77 mmol) was added and the reaction mixture was refluxed for 5 h. The volatile materials were then removed by rotary evaporator and the residue was triturated with hexane, which yielded yellow needles of crude 9-chloromethylanthracene (~95%). This intermediate was dissolved in dry dioxane (20 ml) and 2-(*N*-methylamino)ethanol (1.2 ml, 15 mmol) was added. The reaction mixture was refluxed for 24 h. The crude material obtained after aqueous dichloromethane work up was silica gel column chromatographed (0-6%EtOH:CH_2Cl_2). Yield 1.2 g, 80%. R_f: 0.45 (A); ^{1}H-NMR ($CDCl_3$): 8.40 (m, 3H) arom.; 7.98 (d, 2H) arom.; 7.54-7.41(m, 4H) arom.; 4.52 (s, 2H) 9-CH_2; 3.53 (t, J = 5.4Hz, 2H) -CH_2OH; 2.70 (t, 2H) -CH_2CH$_2$OH; 2.53 (br, 1H) OH; 2.32 (s, 3H) -NCH_3; ^{13}C-NMR ($CDCl_3$): 131.3, 131.1, 129.4, 129.1, 127.7, 125.8, 124.7, 124.4, (arom.); 58.2 (anthracene-9-$\underline{C}H_2$); 57.9 (C2); 53.9(C1); 41.1 (N-$\underline{C}H_3$).

9-(N-(2-hydroxyethyl)-N-methyl)aminofluorene (11).

9-bromofluorene (1.22 g, 5 mmol) was dissolved in dichloromethane (40 ml). Then 2-(*N*-methylamino)ethanol (0.8 ml, 10 mmol) was added and the reaction mixture was stirred for 3 h. The crude material obtained after aqueous dichloromethane work up was silica gel column chromatographed (0-2%EtOH:CH_2Cl_2). Yield 958 mg, 80%. R_f: 0.45 (A); ^{1}H-NMR ($CDCl_3$): 7.69 (d, 2H) arom.; 7.59 (d, 2H) arom.; 7.41-7.26 (m, 4H) arom.; 4.86 (s, 1H) fluorene-CH; 3.59 (t, J = 5.5Hz, 2H) -CH_2OH; 2.80 (t, 2H) -NCH_2CH$_2$OH; 2.80 (br, 1H) OH; 2.23 (s, 3H) -NCH_3; ^{13}C-NMR ($CDCl_3$): 143.6, 140.8, 128.1, 127.0, 125.3, 119.7 (arom.); 70.1 (fluorene-$\underline{C}$H); 58.0 (C2); 55.6 (C1); 36.8 (N-$\underline{C}H_3$).

Mono nitro 9-(2-hydroxyethoxy)phenanthrene (2) and mono nitro 1-(4-hydroxybutyl)pyrene (5).

The free hydroxyl group of **1** and **4** (1-(4-hydroxybutyl)pyrene) were acetylated using acetic anhydride (10 eq) in pyridine (10ml/mmol). After standard workup by aqueous sodium bicarbonate and dichloromethane, the resulting crude acetylated intermediate (>98% purity) was stirred in acetic anhydride (6 ml/mmol) at 0° C. To the resulting emulsion, a solution of 65% HNO_3 (150 µl/mmol) in acetic anhydride (500 µl/mmol)[14] was added dropwise during 30 min, which gave a clear orange solution. After additional stirring for 30 min at 0°C, the solution was poured into ice cold $NaHCO_3$ solution and extracted by dichloromethane. Following concentration and coevaporation by toluene, the residue was treated with 0.4 M NaOH in ethanol for 1h. This was followed by aqueous dichloromethane workup. The residue obtained was subjected to silica gel chromatography (1%-6%EtOH / CH_2Cl_2) to give **2** (321 mg (1.13 mmol), 90%, from 300 mg (1.26 mmol) of **1**) and **5** (111 mg (0.35 mmol), 95%, from 100 mg (0.36 mmol) of **4**). Spectroscopic data for **2**: R_f: 0.40 (A); ^{1}H-NMR ($CDCl_3$): 9.50 (d) arom.; 8.88 (d) arom.; 8.70 (m) arom.; 8.46-8.30 (m) arom.; 8.22 (d) arom.; 7.86-

7.67 (m) arom.; 7.26 (s, 60%, isom. 1) H10 ; 7.06 (s, 40% isom. 2) H10; (4.43 (t) 60%, isom. 1; 4.39 (t) 40%, isom. 2) 2H, 1-CH_2-; (4.20 (m) 60%, isom. 1; 4.07 (m), 40%, isom. 2) 2H, 2-CH_2; (2.24 (t), 40%, isom. 2; 2.06 (t), 60%, isom. 1) 1H, OH. ^{13}C-NMR ($CDCl_3$): 135.2-119.0 (arom. 22 peaks from 3-mono nitro isomers); 69.8, 69.2, 68.4 (C1); 63.4, 63.1, 62.9 (C2); Spectroscopic data for **5**: R_f: 0.30 (A); ^{1}H-NMR ($CDCl_3$): 8.67-7.73 (m, 8H) arom.; 3.72 (br, 2H) 4-CH_2; (3.25 (m), 67%, 2 isomers; 3.13 (t), 33%, 1 isomer) 2H, 1-CH_2-; 1.95-1.65 (m, 5H) -CH_2CH_2- & OH; ^{13}C-NMR ($CDCl_3$): 142.0-120.2 (arom. 31 peaks from 3-mono nitro isomers); 62.4 (C4, 67%), 62.3 (C4, 33%); 33.1, 32.9, 32.6, 32.5, 28.0, 27.0 (C1, C2, C3, from 3-isomers).

*Synthesis of 3'-O-(9--9-yl)thymidine -5'-(O-(2-cyanoethyl))-(O-chromophore-alkyl)phosphates (**14a-22a**).*

General procedure.[11a] 3'-*O*-(9-phenylxanthen-9-yl)thymidine-5'-(*O*-(2-cyanoethyl))-(*N,N*-diisopropyl) phosphoamidite **12** or **13** (1.2 eq.) and hydroxyalkylchromophore (**1-11**) (1 eq.) were coevaporated together with dry acetonitrile and then dissolved in dry acetonitrile (6 ml/mmol amidite). Then tetrazole (5 eq.) was added and the resulting reaction solution was stirred under nitrogen for 45 min. Then the reaction was quenched by addition of 0.1M iodine in THF / pyridine / water (7:2:1 v/v/v) (1.3 eq.) and stirred for 10 min. The crude residue obtained after aqueous ammonium bicarbonate / sodium thiosulfate / dichloromethane work up and drying by filtration through Na_2SO_4 was then silica gel column chromatographed. (**12** was prepared by standard phosphitylation[9] of 3'-*O*-(9-phenylxanthen-9-yl)thymidine[32]. **13** was prepared first by acylation of 3'-*O*-(9-phenylxanthen-9-yl)thymidine with 4-(1-octadecyloxy)benzoyl chloride using the transient trimethylsilyl protection method[33], followed by 5'-phosphitylation[9]).

*Compound **14a***. **12** (365 mg, 0.56 mmol), **1** (111 mg, 0.46 mmol), tetrazole (195 mg, 2.78 mmol). Silica gel column chromatography (0-4% EtOH/CH_2Cl_2/1% pyridine). Yield 338 mg (92%). R_f: 0.70 (C); ^{1}H-NMR ($CDCl_3$): 8.67-6.94 (m, 23H) arom. & NH & H6; 6.24 (dd, 1H) H1'; 4.26-4.41 (m, 4H) -OCH_2CH_2O-; 4.11 (m, 2H) -O$CH_2$$CH_2$CN; 3.90 (m, 2H) H3', H4'; 3.80 (m, 1H) H5'; 3.31 (m, 1H) H5"; [2.60 (t, 1/2 x 2H), 2.57 (t, 1/2 x 2H)] -OCH$_2$$CH_2$CN; 1.93 (m, 1H) H2'; 1.80 (m, 3H) 5-CH_3; 1.44 (m, 1H) H2". ^{31}P-NMR ($CDCl_3$): -1.66, -1.86 ppm.

*Compound **15a***. **12** (526 mg, 0.8 mmol), **2** (190 mg, 0.67 mmol), tetrazole (235 mg, 3.35 mmol). Silica gel column chromatography (0-2% EtOH/CH_2Cl_2/1% pyridine). Yield 470 mg (75%). R_f: 0.65 (C); ^{1}H-NMR ($CDCl_3$): 9.50 (d) arom.; 8.88 (d) arom.; 8.73 (m) arom.; 8.44-8.00 (m) arom.; 7.89-7.66 (m) arom.; 7.45-6.97 (m) arom., H6, total 22H; (6.30 (m) 40% isom. 2); 6.24 (m) 60% isom. 1) 1H, H1'; 4.62-4.31 (m, 4H) -OCH_2CH_2O-; 4.28-4.07 (m, 2H) -OCH_2CH$_2$CN; 4.03-3.74 (m, 3H) H3', H4', H5'; 3.36 (m, 1H) H5"; (2.74 (m) 40% isom. 2; 2.65 (m) 60% isom. 1) 2H, -OCH$_2$$CH_2$CN; 1.95 (m, 1H) H2'; 1.83, 1.81 (2 x s, 3H) 5-CH_3; 1.49 (m, 1H) H2". ^{31}P-NMR ($CDCl_3$): -1.56, -1.68, -1.88, -1.98, -2.12 ppm.

*Compound **16a***. **12** (393 mg, 0.6 mmol), **3** (133 mg, 0.5 mmol), tetrazole (175 mg, 2.5 mmol). Silica gel column chromatography (0-1% EtOH/CH_2Cl_2/1% pyridine). Yield 184 mg (45%). R_f: 0.80 (C); ^{1}H-NMR ($CDCl_3$): 9.40 (br, 1H) NH; 8.62 (d, 1H) arom.; 8.55 (d, 1H) arom.; 8.34 (m, 1H) arom.; 7.80-6.9i (m, 19H) arom., H6; 6.30 (dd, 1H) H1'; 4.24 (m, 2H) POCH$_2$$CH_2$O-; 4.11 (m, 4H) -O$CH_2CH_2CN, POCH_2CH_2$O-; 3.90 (m, 2H) H3', H4'; 3.74 (m, 1H) H5'; 3.27 (m, 1H) H5"; 2.60 (m, 2H) -OCH$_2$$CH_2$CN; 1.95 (m, 1H) H2'; 1.83 (m, 3H) 5-CH_3; 1.46 (m, 1H) H2". ^{31}P-NMR ($CDCl_3$): -1.85 ppm.

*Compound **17a***. **12** (365 mg, 0.56 mmol), **6** (117 mg, 0.46 mmol), tetrazole (195 mg, 2.78 mmol). Silica gel column chromatography (0-6% EtOH/CH_2Cl_2/1% pyridine). Yield 344 mg (92%). R_f: 70 (C); ^{1}H-NMR ($CDCl_3$): 8.25 (br, 1H) NH; 8.17-7.00 (m, 21H) arom. & & H6; 6.21 (m, 1H) H1'; 4.25 (m, 2H) POCH_2CH$_2$N-; 4.03 (m, 2H) -OCH_2CH$_2$CN; 3.82 (m, 4H) H3', H4' & POCH$_2$$CH_2$N-; 3.66 (m, 1H) H5'; 3.26 (m, 1H) H5"; 3.22, 3.19 (2 x s, 3H) N-CH$_3$; 2.60 (m, 2H) -OCH$_2$$CH_2$CN; 1.91 (m, 1H) H2'; 1.83 (m, 3H) 5-CH$_3$; 1.38 (m, 1H) H2". ^{31}P-NMR ($CDCl_3$): -1.71, -1.81 ppm.

*Compound **18a***. **13** (574 mg, 0.56 mmol), **7** (273 mg, 0.67 mmol), tetrazole (197 mg, 2.79 mmol). Silica gel column chromatography (0-4% EtOH/CH_2Cl_2/1% pyridine). Yield 184 mg (45%). R_f: 0.40 (C); ^{1}H-NMR ($CDCl_3$): 8.31-6.88 (m, 25H) arom. & H6; 6.21 (m, 1H) H1'; 5.26 (m, 2H) 9-CH_2CH$_3$; 4.48 (br, 3H) N-CH_3; 4.49 (m, 2H) -OCH_2CH$_2$CN; 4.02-3.39 (m, 8H) H3', H4', H5', H5", -OCH_2CH_2N-; 2.78 (m, 2H) -OCH$_2$$CH_2$CN; 2.00 (m, 1H) H2'; 1.87 (m, 3H) 5-CH_3; 1.70 (t, 3H) 9-CH$_2$$CH_3$; 1.56 (m, 1H) H2"; 1.27 (m, 34H) CH$_3$$C_{17}H_{34}$O-; 0.87 (t, 3H) CH_3C$_{17}H_{34}$O-. ^{31}P-NMR ($CDCl_3$): -2.03, -2.37 ppm.

*Compound **19a***. **12** (424 mg, 0.65 mmol), **8** (102 mg, 0.54 mmol), tetrazole (189 mg, 2.7 mmol). Silica gel column chromatography (0-3% EtOH/CH_2Cl_2/1% pyridine). Yield 376 mg (92%). R_f: 0.90 (C); ^{1}H-NMR

($CDCl_3$): 8.23 (m, 1H) arom.; 7.90 (br, 1H) NH; 7.81 (d, 1H) arom.; 7.54-6.96 (m, 17H) arom., H6; 6.77 (t, 1H) arom.; 6.26 (dd, 1H) H1'; 4.49 (m, 2H) -OC$H_2$$CH_2$OP; 4.32 (m, 2H) -$OCH_2CH_2$OP; 4.08 (m, 2H) -OC$H_2$$CH_2$CN; 3.89 (m, 2H) H3', H4'; 3.77 (m, 1H) H5'; 3.29 (m, 1H) H5"; 2.57 (m, 2H) -OCH_2CH_2CN; 1.91 (m, 1H) H2'; 1.81 (m, 3H) 5-*CH_3*; 1.47 (m, 1H) H2". ^{31}P-NMR ($CDCl_3$): -1.69, -1.86 ppm.

Compound ***20a***. **12** (338 mg, 0.52 mmol), **9** (81 mg, 0.43 mmol), tetrazole (150 mg, 2.15 mmol). Silica gel column chromatography (0-3% EtOH/CH_2Cl_2/1% pyridine). Yield 282 mg (87%). R_f: 0.90 (C); ^{1}H-NMR ($CDCl_3$): 7.99 (s, 1H) NH; 7.79-7.01 (m, 21H) arom. & H6; 6.28 (dd, 1H) H1'; 4.38 (m, 2H) -OC$H_2$$CH_2$OP; 4.28 (m, 2H) -$OCH_2CH_2$OP; 4.15 (m, 2H) -OC$H_2$$CH_2$CN; 3.95 (m, 1H) H4', 3.99 (m, 1H) H3'; 3.80 (m, 1H) H5'; 3.31 (m, 1H) H5"; [2.68 (t, J = 6.6Hz, 1/2 x 2H), 2.66 (t, J = 6.3Hz, 1/2 x 2H)] -OC$H_2$$CH_2$CN; 1.95 (m, 1H) H2'; 1.83 (m, 3H) 5-*CH_3*; 1.46 (m, 1H) H2". ^{31}P-NMR ($CDCl_3$): -1.78, -1.95 ppm.

Compound ***21a***. **12** (393 mg, 0.6 mmol), **10** (126 mg, 0.5 mmol), tetrazole (210 mg, 3.0 mmol). Silica gel column chromatography (0-4% EtOH/CH_2Cl_2/1% pyridine). Yield 184 mg (45%). R_f: 0.60 (C); ^{1}H-NMR ($CDCl_3$): 8.45-6.90 (m, 24H) arom. & NH & H6; 6.24 (m, 1H) H1'; 4.48, 4.46 (2 x s, 2H) anthracene-9-*CH_2*-; 4.07-3.90 (m, 2H) H3', H4'; 3.78 (m, 4H) -OC$H_2$$CH_2$CN & -OC$H_2$$CH_2$N-; 3.59 (m, 1H) H5'; 3.07 (m, 1H) H5"; 2.78 (m, 2H), -OCH_2CH_2CN; 2.38 (m, 2H) -OCH_2CH_2N; 2.39, 2.37 (2 x s, 3H) N-CH_3; 1.89 (m, 1H) H2'; 1.80 (m, 3H) 5-CH_3; 1.36 (m, 1H) H2". ^{31}P-NMR ($CDCl_3$): -1.95 ppm.

Compound ***22a***. **12** (393 mg, 0.6 mmol), **11** (119 mg, 0.5 mmol), tetrazole (210 mg, 3.0 mmol). Silica gel column chromatography (0-3% EtOH/CH_2Cl_2/1% pyridine). Yield 245 mg (62%). R_f: 0.85 (C); ^{1}H-NMR ($CDCl_3$): 8.17 (br, 1H) NH; 7.71-6.99 (m, 22H) arom. & H6; 6.30 (dd, 1H) H1'; 4.84, 4.82 (2 x s, 1H) *CH*; 4.13-3.38 (m, 6H) H3', H4', -OC$H_2$$CH_2$CN & -OC$H_2$$CH_2$N-; 3.73 (m, 1H) H5'; 3.20 (m, 1H) H5"; 2.69-2.61 (m, 4H) -OCH_2CH_2CN & -OCH_2CH_2N-; 2.44, 2.40 (2 x s, 3H) N-*CH_3*; 1.94 (m, 1H) H2'; 1.79 (m, 3H) 5-*CH_3*; 1.44 (m, 1H) H2". ^{31}P-NMR ($CDCl_3$): -1.73, -1.83 ppm.

*Synthesis of thymidine -5'-(O-(2-cyanoethyl))-(O-chromophore-alkyl)phosphates (**14b-22b**). General procedure.* [15a,b]

The 3'-*O*-(9-phenylxanthen-9-yl) thymidine-5'-(*O*-(2-cyanoethyl))-(*O*-chromophore-alkyl)phosphate (**14a-22a**) (1 eq.) was dissolved in a solution of 2% methanol in dichloromethane (half of the required amount) and cooled to 0°C in a ice-bath. Trichloroacetic acid (15 eq.) was dissolved in the solution of 2% methanol in dichloromethane (second half of the required amount), cooled to 0°C and then poured into the solution of (**14a-22a**). The final acid concentration was 0.08M. After complete removal of the 9-phenylxanthen-9-yl group, usually within 2-3 h, the reaction was quenched with pyridine (~30 eq.). The reaction mixture was then worked up by aqueous ammonium bicarbonate-dichloromethane extraction (x4), followed by drying of the organic phase by filtration through Na_2SO_4 and the residue obtained after evaporation was then silica gel column chromatographed.

Compound ***14b***. The 3'-*O*-(9-phenylxanthen-9-yl) block **14a** (338 mg, 0.48 mmol), TCA (1.05 mg, 6.4 mmol). Silica gel column chromatography (0-6% EtOH/CH_2Cl_2). Yield 176 mg (71%). R_f: 0.35 (C); ^{1}H-NMR ($CDCl_3$): 8.71-8.56(m, 4H) arom. & NH; 8.56(t, 1H) arom.; 7.76-7.50 (m, 5H) arom.; 7.25 (s, 1H) H6; 6.96 (s, 1H) arom. H10; 6.17 (m, 1H) H1'; 4.66 (m, 3H) H3', -OC$H_2$$CH_2$OP; 4.49-4.12 (m, 6H) -$OCH_2CH_2$OP, -OC$H_2$$CH_2$CN, H5'; H5"; 4.00 (m, 1H) H4'; 3.02 (br, 1H) OH; 2.66 (m, 2H) -OCH_2CH_2CN; 2.23 (m, 1H) H2'; 2.07 (m, 1H) H2"; 1.88 (m, 3H) 5-*CH_3*. ^{31}P-NMR ($CDCl_3$): -1.17, -1.32 ppm.

Compound ***15b***. The 3'-*O*-(9-phenylxanthen-9-yl) block **15a** (470 mg, 0.55 mmol), TCA (1.35 g, 8.26 mmol). Silica gel column chromatography (0-5% EtOH/CH_2Cl_2). Yield 200 mg (56%). R_f: 0.30 (C); ^{1}H-NMR ($CDCl_3$): 9.51 (d) arom.; 8.93 (d) arom.; 8.74 (m) arom.; 8.48-8.23 (m) arom.; 7.89-7.69 (m) arom.; 7.35 (m, 1H) H6, total 9H; (7.25 (s) 60% isom.1; 7.07 (s) 40% isom. 2) 1H, H10; (6.29 (m) 40% isom. 2); 6.20 (m) 60% isom. 1) 1H, H1'; 4.70 (m, 1H) H3'; 4.62-4.24 (m, 6H) -OCH_2CH_2OP, H5', H5"; 4.15-3.98 (m, 1H) H4'; 2.77 (m, 2H) -OCH_2CH_2CN; 2.42-2.10 (m, 2H) H2', H2"; 1.88 (m, 3H) 5-*CH_3*. ^{31}P-NMR ($CDCl_3$): -1.00, -1.37, -1.54, -1.64, -1.76 ppm.

Compound ***16b***. The 3'-*O*-(9-phenylxanthen-9-yl) block **16a** (390 mg, 0.6 mmol), TCA (1.14 g, 6.99 mmol). Silica gel column chromatography (0-5% EtOH/CH_2Cl_2). Yield 240 mg (82%). R_f: 0.40 (C); ^{1}H-NMR ($CDCl_3$): 8.66-8.55(m, 3H) arom.; 8.33 (m, 1H) arom.; 7.77-7.46 (m, 5H) arom.; 7.28 (s, 1H) H6; 6.97 (s, 1H) arom. H10; 6.22 (m, 1H) H1'; 4.46 (m, 1H) H3'; 4.36-4.17 (m, 8H) -$OCH_2CH_2CH_2CH_2$OP, -OC$H_2$$CH_2$CN, H5'; H5"; 4.02 (m, 1H) H4'; 3.08 (br, 1H) OH; 2.70 (m, 2H) -OCH_2CH_2CN; 2.32 (m, 1H) H2'; 2.16 (m, 1H)

H2"; 2.08 (m, 4H) -OCH$_2$*CH$_2$CH$_2$*CH$_2$OP; 1.91 (m, 3H) 5-*CH$_3$*. ^{31}P-NMR ($CDCl_3$): -1.05, -1.37 ppm.

Compound ***17b***. The 3'-*O*-(9-phenylxanthen-9-yl) block **17a** (344 mg, 0.43 mmol), TCA (1.04 g, 6.39 mmol). Silica gel column chromatography (0-8% EtOH/CH_2Cl_2). Yield 187 mg (74%). R_f: 0.35 (C); ^{1}H-NMR ($CDCl_3$+CD_3OD): 8.16-8.05 (m, 3H) arom.; 7.82-7.64 (m, 3H) arom.; 7.23, 7.22 (2 x s, 1H) H6; 7.15, 7.14 (2 x s, 1H) H1; 6.15 (dd, $J_{1',2'}$ = 6.6Hz, $J_{1',2''}$ = 6.2Hz, 1H) H1'; 4.44-4.31 (m, 3H) POC*H$_2$*CH$_2$N-, H3'; 4.25-4.15 (m, 4H) -OC*H$_2$*CH$_2$CN, H5', H5"; 4.02-3.89 (m, 3H) H4' & POCH$_2$C*H$_2$*N-; 3.27, 3.26 (2 x s, 3H) N-*CH$_3$*; 2.71 (m, 2H) -OCH$_2$C*H$_2$*CN; 2.29 (m, 1H) H2'; 2.11 (m, 1H) H2"; 1.87 (m, 3H) 5-*C H$_3$*. ^{31}P-NMR ($CDCl_3$+CD_3OD): -1.44, -1.61 ppm.

Compound ***18b***. The 3'-*O*-(9-phenylxanthen-9-yl) block **18a** (617 mg, 0.48 mmol, (HCO_3^-)), TCA (1.57 g, 9.6 mmol). Silica gel column chromatography (5-30% EtOH/CH_2Cl_2). Yield 443 mg (HCO_3^-), (86%). R_f: 0.20 (C); ^{1}H-NMR ($CDCl_3$+CD_3OD): 8.32 (d, 1H) arom.; 8.10 (m, 4H) arom.; 7.82 (d, 2H) Bz; 7.81 (m, 1H) arom.; 7.44 (s, 1H) H6; 7.20 (br, 1H) H1; 6.92 (d, 2H) Bz; 6.13 (m, 1H) H1'; 5.15 (m, 2H) 9-*CH$_2$*CH$_3$; 4.60 (br, 3H) N-*CH$_3$*; 4.50-4.22 (m, 8H) -O*CH$_2$*CH$_2$CN, -O*CH$_2$*CH$_2$N-, H3', H4', H5', H5"; 4.00 (t, 2H) -OCH$_2$*CH$_2$*N-; 2.80 (m, 2H) -OCH$_2$*CH$_2$*CN; 2.34 (m, 2H) H2', H2"; 1.92 (m, 3H) 5-*CH$_3$*; 1.69 (t, 3H) 9-CH$_2$*CH$_3$*; 1.27 (m, 34H) CH$_3$*C$_{17}$H$_{34}$*O-; 0.87 (t, 3H) *CH$_3$*C$_{17}$H$_{34}$O-. ^{31}P-NMR ($CDCl_3$+CD_3OD): -2.03, -2.12 ppm.

Compound ***19b***. The 3'-*O*-(9-phenylxanthen-9-yl) block **19a** (450 mg, 0.59 mmol), TCA (1.46 g, 8.9 mmol). Silica gel column chromatography (0-6% EtOH/CH_2Cl_2). Yield 268 mg (83%). R_f: 0.30 (C); ^{1}H-NMR ($CDCl_3$): 8.77 (s, 1H) NH; 7.78-7.10 (m, 8H) arom. & H6; 6.24 (dd, 1H) H1'; 4.57-4.46 (m, 3H) H3', -O*CH$_2$*CH$_2$OP; 4.38-4.26 (m, 6H) -OCH$_2$C*H$_2$*OP, -O*CH$_2$*CH$_2$CN, H5', H5"; 4.06 (m, 1H) H4'; 3.27 (br, 1H) OH; 2.75 (m, 2H) -OCH$_2$C*H$_2$*CN; 2.33 (m, 1H) H2'; 2.18 (m, 1H) H2"; 1.91 (m, 3H) 5-*CH$_3$*. ^{31}P-NMR ($CDCl_3$): -1.25, -1.42 ppm.

Compound ***20b***. The 3'-*O*-(9-phenylxanthen-9-yl) block **20a** (282 mg, 0.37 mmol), TCA (912 mg, 5.58 mmol). Silica gel column chromatography (0-6% EtOH/CH_2Cl_2). Yield 134 mg (66%). R_f: 0.35 (C); ^{1}H-NMR ($CDCl_3$): 9.92 (br, 1H) NH; 8.25 (m, 1H) arom.; 7.75 (m, 1H) arom.; 7.50-7.22 (m, 5H) arom., H6; 6.75 (m, 1H) arom.; 6.23 (dd, 1H) H1'; 4.56 (m, 2H) -O*CH$_2$*CH$_2$OP; 4.40-4.16 (m, 6H) -OCH$_2$C*H$_2$*OP, -O*CH$_2$*CH$_2$CN, H5', H5"; 4.06 (m, 1H) H4'; 2.60 (t, 2H) -OCH$_2$C*H$_2$*CN; 2.50 (br, 1H) OH; 2.27 (m, 1H) H2'; 2.06 (m, 1H) H2"; 1.84 (m, 3H) 5-*CH$_3$*. ^{31}P-NMR ($CDCl_3$): -1.39, -1.54 ppm.

Compound ***21b***. The 3'-*O*-(9-phenylxanthen-9-yl) block **21a** (184 mg, 0.22 mmol), TCA (549 mg, 3.36 mmol). Silica gel column chromatography (0-6% EtOH/CH_2Cl_2). Yield 85 mg (63%). R_f: 0.35 (C); ^{1}H-NMR ($CDCl_3$): 9.27 (br, 1H) NH; 8.41 (m, 3H) arom.; 7.98 (d, 2H) arom.; 7.53-7.42 (m, 4H) arom.; 7.24 (s, 1H) H6; 6.2o (dd, 1H) H1'; 4.47 (s, 2H) anthracene-9-*CH$_2$*-; 4.31 (m, 1H) H3'; 4.20-3.86 (m, 7H) H4', -O*C H$_2$*CH$_2$CN, -O*CH$_2$*CH$_2$N-, H5', H5"; 2.85 (m, 2H), -OCH$_2$C*H$_2$*CN; 2.46 (m, 2H) -OCH$_2$C*H$_2$*N; 2.37 (s, 3H) N-*CH$_3$*; 2.24 (m, 1H) H2'; 1.99 (m, 1H) H2"; 1.82 (m, 3H) 5-*CH$_3$*. ^{31}P-NMR ($CDCl_3$): -1.58 ppm.

Compound ***22b***. The 3'-*O*-(9-phenylxanthen-9-yl) block **22a** (226 mg, 0.29 mmol), TCA (698 mg, 4.28 mmol). Silica gel column chromatography (0-6% EtOH/CH_2Cl_2). Yield 140 mg (85%). R_f: 0.45 (C); ^{1}H-NMR ($CDCl_3$): 8.87 (br, 1H) NH; 7.69 (d, 4H) arom.; 7.42-7.26 (m, 5H) arom. & H6; 6.21 (dd, 1H) H1'; 5.02 (s, 1H) *CH*; 4.52 (m, 1H) H3'; 4.33 (m, 2H) H5', H5"; 4.22 (m, 4H) -O*CH$_2$*CH$_2$CN & -O*CH$_2$*CH$_2$N-; 4.07(m, 1H) H4'; 2.86-2.72 (m, 4H) -OCH$_2$C*H$_2$*CN & -OCH$_2$C*H$_2$*N-; 2.65 (br, 1H) OH; 2.56, 2.54 (2 x s, 3H) N-*CH$_3$*; 2.39 (m, 1H) H2'; 2.20 (m, 1H) H2"; 1.88, 1.86 (2 x s, 3H) 5-*CH$_3$*. ^{31}P-NMR ($CDCl_3$): -1.46, -1.56 ppm.

*Synthesis of 5'-(O-(2-cyanoethyl))-(O-chromophore-alkyl)phosphothymidine-3'-(2-cyanoethyl)-(N,N-diisopropyl)phosphoramidite) (**14c-18c, 20c-22c**).*

General procedure.[9] The 3'-hydroxy block (**14b-17b, 19b-22b**) (1 eq.) was dissolved in dry tetrahydrofuran (4 ml/mmol of **14b-17b, 19b-22b**). To this dry diisopropylethylamine (3 eq.) was added, followed by addition of *O*-(2-cyanoethyl)-*N,N*-diisopropylphosphoramidic chloride (2 eq.) under vigorous stirring under nitrogen. After 45 min the reaction was quenched by addition of dry MeOH (10 eq.) and stirred for an additional 15 min. The crude material obtained after aqueous saturated NaCl / ethyl acetate work up and drying by filtration through Na_2SO_4 was then silica gel column chromatographed.

Compound ***14c***. The 3'-hydroxy block **14b** (176 mg, 0.3 mmol). Silica gel column chromatography (EtOH/hexane/CH_2Cl_2 + 5% lutidine, 0/100/100 to 1/0/100, v/v/v). Yield 201 mg (85%). R_f: 0.60 (C); ^{1}H-NMR ($CDCl_3$): 8.66-8.36(m, 3H) arom.; 7.77-7.51 (m, 5H) arom.; 7.35 (m, 1H) H6; 6.98 (s, 1H) H10; 6.25 (m, 1H) H1'; 4.68 (m, 2H) -O*CH$_2$*CH$_2$OP-; 4.49 (m, 3H) H3', -OCH$_2$C*H$_2$*OP-; 4.37-4.13 (m, 7H) 2 x

-O*CH*$_2$CH$_2$CN, H4', H5'; H5"; 3.81-3.49 (m, 4H) 2 x*CH*; -O*CH*$_2$CH$_2$CN; 2.67 (m, 2H) -OCH$_2$*CH*$_2$CN; 2.57 (m, 2H) -OCH$_2$*CH*$_2$CN; 2.35 (m, 1H) H2'; 2.10 (m, 1H) H2"; 1.90 (m, 3H) 5-*CH*$_3$; 1.14 (m, 12H) 4 x *CH*$_3$. ^{31}P-NMR (CDCl$_3$): +149.9, +149.6, +149.4, +149.2, -1.28, -1.46 ppm.

Compound ***15c***. The 3'-hydroxy block **15b** (200 mg, 0.31 mmol). Silica gel column chromatography (EtOH/hexane/CH_2Cl_2 + 5% lutidine, 0/20/80 to 2/0/100, v/v/v). Yield 224 mg (86%). R_f: 0.50 (C); ^{1}H-NMR (CDCl$_3$): 9.48 (s) arom.; 8.89 (d) arom.; 8.71 (m) arom.; 8.52-8.17 (m) arom.; 7.88-7.67 (m) arom.; 7.47-7.31 (m, 1H) H6, total 10H; (6.32 (m, 1H) H1'; 5.05 (m, 1H) H3'; 4.79-3.95 (m, 7H) -O*CH*$_2$*CH*$_2$OP, H4', H5', H5"; 3.94-3.31 (m, 4H) 2 x*CH*; -O*CH*$_2$CH$_2$CN; 2.86-2.56 (m, 4H) 2x-OCH$_2$*CH*$_2$CN; 2.47-2.15 (m, 2H) H2', H2"; 1.91 (m, 3H) 5-*CH*$_3$; 1.33-1.11 (m, 12H) 4 x *CH*$_3$. ^{31}P-NMR (CDCl$_3$): +149.1, -2.10 ppm.

Compound ***16c***. The 3'-hydroxy block **16b** (230 mg, 0.37 mmol). Silica gel column chromatography (0-1% EtOH/CH_2Cl_2/5% lutidine). Yield 240 mg (79%). R_f: 0.70 (C); ^{1}H-NMR (CDCl$_3$): 8.69-8.53(m, 2H) arom.; 8.34 (m, 2H) NH, arom.; 7.81-7.44 (m, 5H) arom.; 7.38 (m, 1H) H6; 6.97 (s, 1H) arom. H10; 6.30 (m, 1H) H1'; 4.57 (m, 1H) H3'; 4.49-4.13 (m, 8H) -O*CH*$_2$CH$_2$CH$_2$*CH*$_2$OP, -O*CH*$_2$CH$_2$CN, H5'; H5"; 4.12-3.24 (m, 5H) H4', 2 x *CH*, -O*CH*$_2$CH$_2$CN; 2.71-262 (m, 4H) 2 x -OCH$_2$*CH*$_2$CN; 2.47 (m, 1H) H2'; 2.17 (m, 1H) H2"; 2.08 (m, 4H) -OCH$_2$*CH*$_2$*CH*$_2$CH$_2$OP; 1.94 (m, 3H) 5-*CH*$_3$; 1.30-1.14 (m, 12H) 4 x *CH*$_3$. ^{31}P-NMR (CDCl$_3$): +148.3, -2.58 ppm.

Compound ***17c***. The 3'-hydroxy block **17b** (187 mg, 0.32 mmol). Silica gel column chromatography (EtOH/hexane/CH_2Cl_2 + 5% lutidine, 0/50/50 to 2/0/100, v/v/v). Yield 163 mg (65%). R_f: 0.55 (C); ^{1}H-NMR (CDCl$_3$): 8.16-8.06 (m, 3H) arom.; 7.78-7.60 (m, 3H) arom.; 7.31 (m, 1H) H6; 7.14, 7.12 (2 x s, 1H) H1; 6.23 (m, 1H) H1'; 4.52 (m, 1H) H3'; 4.39 (m, 2H) PO*CH*$_2$CH$_2$N-; 4.31-4.10 (m, 5H) -O*CH*$_2$CH$_2$CN, H4', H5', H5"; 3.89 (m, 2H) POCH$_2$*CH*$_2$N-; 3.86-3.51 (m, 4H) -O*CH*$_2$CH$_2$CN, 2 x *CH*; 3.25, 3.23 (2 x s, 3H) N-*CH*$_3$; 2.65 (m, 4H) 2 x -OCH$_2$*CH*$_2$CN; 2.41 (m, 1H) H2'; 2.16 (m, 1H) H2"; 1.91 (m, 3H) 5-*CH*$_3$; 1.15 (m, 12H) 4 x *CH*$_3$. ^{31}P-NMR (CDCl$_3$): +149.5, +149.2, +149.1, -1.28, -1.52 ppm.

Compound ***19c***. The 3'-hydroxy block **19b** (268 mg, 0.49 mmol). Silica gel column chromatography (EtOH/hexane/CH_2Cl_2 + 5% lutidine, 0/50/50 to 1/0/100, v/v/v). Yield 200 mg (55%). R_f: 0.80 (C); ^{1}H-NMR (CDCl$_3$): 8.28 (m, 2H) arom., NH; 7.79 (m, 1H) arom.; 7.52-7.33 (m, 5H) arom. & H6; 6.81 (m, 1H) arom.; 6.29 (m, 1H) H1'; 4.70-4.49 (m, 3H) H3', -O*CH*$_2$CH$_2$OP; 4.44-4.12 (m, 7H) -OCH$_2$*CH*$_2$OP, -O*CH*$_2$CH$_2$CN, H5', H5", H4'; 3.88-3.50 (m, 4H) 2 x *CH*, -O*CH*$_2$CH$_2$CN; 2.70-2.53 (m, 4H) 2 x -OCH$_2$*CH*$_2$CN; 2.40 (m, 1H) H2'; 2.11 (m, 1H) H2"; 1.90 (m, 3H) 5-*CH*$_3$; 1.18 (m, 12H) 4 x *CH*$_3$. ^{31}P-NMR (CDCl$_3$): +149.5, +149.2, -1.34, -1.60 ppm.

Compound ***20c***. The 3'-hydroxy block **20b** (134 mg, 0.25 mmol). Silica gel column chromatography (EtOH/hexane/CH_2Cl_2 + 5% lutidine, 0/50/50 to 1/0/100, v/v/v). Yield 147 mg (80%). R_f: 0.80 (C); ^{1}H-NMR (CDCl$_3$): 8.48 (br, 1H) NH; 7.78-7.10 (m, 8H) arom. & H6; 6.32 (m, 1H) H1'; 4.64-4.48 (m, 3H) H3', -O*CH*$_2$CH$_2$OP; 4.44-4.22 (m, 6H) -OCH$_2$*CH*$_2$OP, -O*CH*$_2$CH$_2$CN, H5', H5"; 4.18 (m, 1H) H4'; 3.92-3.52 (m, 4H) 2 x *CH*, -O*CH*$_2$CH$_2$CN; 2.74 (m, 2H) -OCH$_2$*CH*$_2$CN; 2.61 (m, 2H) -OCH$_2$*CH*$_2$CN; 2.42 (m, 1H) H2'; 2.16 (m, 1H) H2"; 1.93 (m, 3H) 5-*CH*$_3$; 1.18 (m, 12H) 4 x *CH*$_3$. ^{31}P-NMR (CDCl$_3$): +149.5, +149.4, +149.3, +149.1, -1.40, -1.58 ppm.

Compound ***21c***. The 3'-hydroxy block **21b** (85 mg, 0.14 mmol). Silica gel column chromatography (EtOH/hexane/CH_2Cl_2 + 5% lutidine, 0/80/20 to 2/0/98, v/v/v). Yield 88 mg (78%). R_f: 0.50 (C); ^{1}H-NMR (CDCl$_3$): 9.00 (br, 1H) NH; 8.46 (m, 3H) arom.; 8.03 (d, 2H) arom.; 7.60-7.52 (m, 4H) arom.; 7.32 (m, 1H) H6; 6.33 (m, 1H) H1'; 4.53 (s, 2H) anthracene-9-*CH*$_2$-; 4.52 (m, 1H) H3'; 4.25-3.90 (m, 7H) H4', -O*CH*$_2$CH$_2$CN, -O*CH*$_2$CH$_2$N-, H5', H5"; 3.86-3.55 (m, 4H) 2 x *CH*, -O*CH*$_2$CH$_2$CN; 2.89 (m, 2H), -OCH$_2$*CH*$_2$CN; 2.63 (m, 2H), -OCH$_2$*CH*$_2$CN; 2.49 (m, 2H) -OCH$_2$*CH*$_2$N; 2.43 (s, 3H) N-*CH*$_3$; 2.40 (m, 1H) H2'; 2.09 (m, 1H) H2"; 1.86 (m, 3H) 5-*CH*$_3$; 1.19 (m, 12H) 4 x *CH*$_3$. ^{31}P-NMR (CDCl$_3$): +149.3, +149.2, +149.1, +148.9, -1.46, -1.77 ppm.

Compound ***22c***. The 3'-hydroxy block **22b** (140 mg, 0.24 mmol). Silica gel column chromatography (EtOH/hexane/CH_2Cl_2 + 5% lutidine, 0/50/50 to 2/0/100, v/v/v). Yield 100 mg (53%). R_f: 0.75 (C); ^{1}H-NMR (CDCl$_3$): 7.69 (d, 2H) arom.; 7.59 (d, 2H) arom.; 7.45-7.28 (m, 3H) arom. & H6; 6.95 (d, 2H) arom.; 6.32 (dd, 1H) H1'; 4.86 (s, 1H) *CH*; 4.57 (m, 1H) H3'; 4.33 (m, 2H) H5', H5"; 4.29-4.10 (m, 4H) -O*CH*$_2$CH$_2$CN & -O*CH*$_2$CH$_2$N-; 4.10 (m, 1H) H4'; 3.86-3.37 (m, 4H) 2 x *CH*, -O*CH*$_2$CH$_2$CN; 2.74-2.63 (m, 6H) 2 x -OCH$_2$*CH*$_2$CN & -OCH$_2$*CH*$_2$N-; 2.44, 2.43 (2 x s, 3H) N-*CH*$_3$; 2.45 (m, 1H) H2'; 2.15 (m, 1H) H2"; 1.88, 1.86 (2 x s, 3H) 5-*CH*$_3$; 1.19 (m, 12H) 4 x *CH*$_3$. ^{31}P-NMR (CDCl$_3$): +149.4, +149.0, -1.28, -1.65 ppm.

Synthesis, deprotection and purification of oligonucleotides **25** - **54** .[5f]

All oligonucleotides were synthesised on 1.0 μmol scale on standard CPG support with an 8-channel Applied Biosystems 392 DNA / RNA synthesiser using conventional β-cyanoethyl phosphoramidite chemistry. The tethered thymidine amidite blocks **14c-17c** and **19c-22c**, as well as the pyrenebutyl amidite blocks **23** and **24**, were dissolved in dry acetonitrile with a final concentration of 0.1M and used for solid-phase synthesis with a coupling time of 75s (25s for standard nucleoside amidites). The coupling efficiency of the tethered amidites, judging from RP-HPLC after deprotection, was in the range 90-99%. The target oligomers **27**, **28**, **41**, **42** and the blank 18-mer **43** were synthesised with "5'-*O*-trityl on". After each synthesis of the protected oligomers **25-35, 37-54** (synthesis of **36** is described separately below), the solid support was transferred directly out from the cassette to a 100 ml RB flask containing 40 ml of conc. aq. NH_3 and was shaken for 2 h at 20°C. After removal of CPG by filtration and the filtrate evaporated, the residue was redissolved in conc. aq. NH_3 and stirred at 55 °C for 16 h. The crude oligomers were purified on reverse-phase HPLC (semi-preparative column Spherisorb 5ODS2) using the following gradient solvents: **A** (0.1M triethylammonium acetate (TEAA), 5% MeCN, pH 7.0; **B** (0.1M triethylammonium acetate, 50% MeCN, pH 7.0). For oligomers **27**, **28**, **41**, **42** and **43** (5'-*O*-DMTr) and **33**, **34**, **47**, **48**, a linear gradient of 0 - 100% buffer **B** over 30 min at a flow of 1 ml / min was used. For oligomers **25, 26, 29-32, 35-40, 44-46, 49-54**, a linear gradient of 0 - 80% buffer **B** over 30 min at a flow of 1 ml / min was used. Retention times (R_t in minutes) of fully deprotected oligomers **25-54** run in respective gradients were as follows: **25** (21.4), **26** (22.1), **27** (30.5(DMTr); 24.8), **28** (29.8(DMTr); 24.4), **29** (20.8), **30** (30.3), **31** (31.1), **32** (30.6), **33** (29.4), **34** (31.7; 32.0; 33.0 from three NO_2-isomers of pyrene), **35** (23.6), **36** (22.4), **37** (26.6), **38** (26.4), **39** (28.0), **40** (27.7), **41** (27.5(DMTr); 23.3), **42** (29.6(DMTr); 25.4), **43** (26.4(DMTr); 20.2), **44** (27.8), **45** (29.4), **46** (29.2), **47** (27.6), **48** (28.0; 28.5 from three NO_2-isomers of phenanthrene), **49** (22.6), **50** (21.0), **51** (25.2), **52** (25.7), **53** (25.8), **54** (26.0).

After collection of the appropriate fractions, the solutions of the 5'-*O*-tritylated oligomers **27**, **28**, **41**, **42** and **43** were evaporated and lyophilised (4 x 1ml H_2O) and then dissolved in 2-3 ml 80% AcOH and stirred for 5 min and then evaporated and neutralised with water / triethylamine, followed by evaporation. The residue was dissolved in water and extracted with diethylether. The water phase was then evaporated and the residue lyophilised (6 x 1 ml H_2O). No second purification was needed. The oligomers **25, 26, 29-40, 44-54** were evaporated and directly lyophilised (7 x 1ml H_2O). All the oligomers were subsequently sodium exchanged through a column of Dowex-50 Na^+-form, the collected solutions evaporated and the A_{260} optical units were determined. A_{260} units (OD) for 1μmol scale: 9-mers **29-40**: 6.0-34.5 OD; Target 10-mer **25**, 45.0 OD; Target 11-mer **26**; 24.5 OD; Target 20-mers **27** & **28**: 36 & 33 OD; Target 24-mer **41**: 40.0 OD; Target 24-mer **42**: 19.5 OD; 18-mers **43-54**: 8.0-60.5 OD.

Synthesis of oligomers **36** *and* **50** *by in situ coupling of compound* ***18b*** *to corresponding CPG bound 5'-hydroxy oligomer.*[10]

18b (25 mg, 23.8 μmol) was coevaporated from dry pyridine in an Eppendorf tube and dissolved in dry pyridine (100 μl). Then a 0.2M acetonitrile solution of *o*-chlorophenylphosphorobistriazolide[16] (120 μl, 1 eq.) was added and the reaction mixture was stirred for 1 h under nitrogen. 1μmol of both 5'-hydroxy oligomers (27 mg CPG, 37 μmol/g) were synthesised on ABI 392 DNA/RNA solid-phase synthesiser (5'-HOd(CCAA ACAT)-CPG (8-mer) for **36** and 5'-HOd(TCT$_6$CT$_6$CT)-CPG (17-mer) for **50**). The dried CPG bound oligomer was in each case removed from the cassette and transferred to an Eppendorf tube and then dry pyridine (~100 μl) was added. To this mixture, the phosphorylation solution of **18b** (~220 μl) and *N*-methylimidazole (16 μl, 16eq.)[34] were added and the resulting mixture was shaken for 24h. The mixture was then filtered and the CPG washed with pyridine, acetonitrile and diethyl ether. The pink coloured CPG was then threated with conc. aq. ammonia for 2 h at 20°C followed by filtration and wash with water. Both of the two pink coloured filtrates (CPG colourless) were evaporated and the residue stirred with conc. aq. ammonia for 24h at 55°C. The residue was purified on semi-preparative RP-HPLC (0-80%**B** in 30 min, 1ml/min) and a pink coloured peak corresponding to **36** and **50** were collected (R_t (min) = **36** (22.4); **50** (21.0)) and lyophilised with water (7 x 0.5 ml) and finally sodium exchanged (Dowex 50 Na+-form). (**36** (3.1 A_{260}-units); **50** (3.8 A_{260}-units)).

Physico-chemical measurements.

Melting measurements.[5f] UV melting profiles were obtained by scanning A_{260} absorbance versus time at a heating rate of 1.0° C / min for duplexes and 0.5° C / min for triplexes. The T_ms were calculated from the culmination point of the first derivative of the melting curves with an accuracy of ±0.1° C. The duplex melting

experiments were carried out in buffer A: 20 mM Na_2HPO_4 / NaH_2PO_4, 0.1M NaCl at pH 7.3 and the triplex melting experiments in buffer A at pH 7.3, 6.5, 6.0 and buffer B: 20 mM Tris HCl, 0.1M NaCl, 20 mM $MgCl_2$ at pH 7.3. The approximate extinction coefficients for oligonucleotides **25** - **54** was calculated as previously described[5f,35]. In the cases of the tethered oligomers (**30-40**, **44-54**), the extinction coefficients were corrected for the absorbance contribution of the aromatic moieties at 260 nm by subtraction.

In a duplex melting measurement, where 1μM of each single strand was used, 1.3 nmol of target sequence (**25**, 0.126 OD / 10 μl H_2O), (**26**, 0.134 OD / 10 μl H_2O) or (**27&28**, 0.25 OD / 10 μl H_2O) and 1.3 nmol of nonamer sequence (0.116 OD / 10 or 20 μl H_2O) were added to 1260 μl of buffer (20.64 mM Na_2HPO_4 / NaH_2PO_4, 0.1032M NaCl, pH 7.3), giving, after dilution with water to 1.3 ml, concentrations of ~1μM of each oligomer and the precise buffer concentration. The solutions were heated to 70° C for 3 min and then allowed to cool down to 20°C for 30 min. The melting curves and dissociation T_m were measured with a temperature gradient 15 - 50° C (35 min) (entries # 1-12, Table 1).

In a triplex melting measurement, where 1μM of each single strand was used, 1.3 nmol of target sequence **41** (0.2 OD / 20 μl H_2O), **42** (0.34 OD / 20 μl H_2O) and 1.3 nmol of octadecamer sequence (0.185 OD / 10 or 20 μl H_2O) were added to 1260 μl of buffer (20.95 mM Na_2HPO_4 / NaH_2PO_4, 0.1047M NaCl, pH 7.3), giving, after dilution with water to 1.32 ml, concentrations of ~1μM of each oligomer and the precise buffer concentration. The solutions were heated to 70° C for 3 min and then allowed to cool down to 20°C for 30 min and then kept at 0° C over night. The melting curves and dissociation T_m were measured with a temperature gradient 5 - 70° C (130 min) (entries # 1-12, Table 2).

In our control experiment, no change in T_m was observed for the tethered oligos in the duplex or triplex form in 0.1M or 1M NaCl in 20mM phosphate buffer. We however observed the increase of T_m for the non-tethered oligos **29** and **25** by ~3° C from 0.1M to 1M NaCl.

Thermodynamics. For the thermodynamic calculations of $\Delta H°$, $\Delta S°$ and $\Delta G°$, T_ms for five different oligonucleotide concentrations (1, 2, 3, 4 and 5 μM total single strand concentration) were measured for the duplexes (9-mers+10-, 11-, 20-mer matched/mismatched) in buffer A at pH 7.3, starting from the highest concentration (5 μM) and then stepwise decreasing the concentration by dilution at the same buffer concentration. Denaturation and renaturation of the samples was carried out prior to each melting measurement as described above. The resulting T_m-values were fitted to a van't Hoff plot of T_m^{-1} vs ln C_T and thermodynamic parameters were calculated.[20]

Fluorescence. For the fluorescence measurements, the concentration of each oligomer mixture (1.3 ml) was set relative to 0.02 abs. units at the chromophores excitation wavelength: **1** (304 nm); **2** (384 nm); **3** (354 nm); **4** (348 nm); **5** (345 nm); **6** (496 nm); **7** (548 nm); **8** (320 nm); **9** (327 nm); **10** (370 nm); **11** (304 nm). The ratio of the single strands in the mixtures of duplexes and triplexes were always 1:1 and 1:1:1 respectively. All measurements were done in 20 mM Na_2HPO_4 / NaH_2PO_4, 1.0M NaCl (at pH 7.3 for duplexes and at pH 6.0 for triplexes). During measurements the temperature was kept at ~22° C by circulating termostated water through the cuvette holder. Relative fluorescence intensities and Stoke's shifts were determined for each sample at the same excitation/emission bandpass width.

ACKNOWLEDGEMENTS

Authors thank Swedish Natural Science Research Council (NFR) and Engineering Research Council (TFR) for generous funding.

REFERENCES

1. (a) Hélène, C. *Eur. J. Cancer* **1991**, *27*, 1466-1471. (b) Matteucci, M.; Bischofberger, N. *Annual Reports in Mecicinal Chemistry* **1991**, *26*, 287-296. (c) Thoung, N. T.; Hélène, C. *Angew. Chem. Int. Ed. Engl.* **1993**, *32*, 666-690. (d) Milligan, J.; Matteucci, M.; Martin, J. *J. Med. Chem.* **1993**, *36*, 1923-1937.
2. (a) Goodchild, J. *Bioconjugate Chemistry* **1990**, *1(3)*, 165-187. (b) Uhlmann, E.; Peyman, A. *Chem. Rev.* **1990**, *90*, 544-584. (c) Asseline, U.; Thoung, N. T.; Hélène, C. *New J. Chem* **1997**. *21*, 5-17.
3. (a) Beaucage, S.; Radhakrishnan, P. *Tetrahedron* **1993**, *49*, 1925-1963. (b) Maltseva, T.; Agback P.; Repkova, M.; Venyaminova, A.; Ivanova, I.; Sandström, A.; Zarytova, V.; Chattopadhyaya, J. *Nucleic Acids Res.* **1994**, *22*, 5590-5599. (c) Knorre, D.G.; Vlassov, V.V.; Zarytova, V.F.; Lebedev,

A.V.; Federova, O.S. *Design and Targeted Reactions of Oligonucleotide Derivatives* , CRC Press: Florida. 1994.
4. (a) Xodo, L.; Manzini, G.; Quadrifoglio, F.; van der Marel, G.; van Boom, J. *Nucleic Acids Res.* **1991**, *19*, 5625-5631. (b) Francois, P.; Muzzin, P.; Dechamps, M.; Sonveaux, E. *New J. Chem.* **1994**, *18*, 649-657. (c) Froehler, B.; Wadwani, S.; Terhorst, T.; Gerrard, S. *Tetrahedron Lett.* **1992**, *33*, 5307-5310.
5. (a) Tung, C.; Breslauer, K.; Stein, S. *Nucleic Acids Res.* **1993**, *21*, 5489-5494. (b) Prakash,T.; Barawkar, D.; Kumar, V.;Ganesh, K. *Bioorg. Med. Chem. Lett.* **1994**, *4*, 1733-1738. (c) Schmid, N.; Behr, J. *Tetrahedron Lett.* **1995**, *36*, 1447-1450. (d) Bigey, P.; Pratviel, G.; Meunier, B. *J. Chem. Soc., Chem. Comm.* **1995**, 181-182. (e) Barawkar, D.; Rajeev, K.; Kumar, V.; Ganesh, K. *Nucleic Acids Res.* **1996**, *24*, 1229-1237. (f) Sund, C.; Puri, N.; Chattopadhyaya, J. *Tetrahedron* **1996**, *52*, 12275-12290.
6. Maltseva, T.; Sandström, A.; Ivanova, I.; Sergeyev, D.; Zarytova, V.; Chattopadhyaya, J. *J. Biochem. Biophys. Methods* **1993**, *26*, 173-236.
7. Hunter, C. *Angew. Chem. Int. Ed. Engl.* **1993**, *32*, 1584-1586.
8. Kato, Y.; Conn, M.; Rebek Jr, J. *Proc. Natl. Acad. Sci.* **1995**, *92*, 1208-1212.
9. Sinha, N.; Biernat, J.; Köster, H. *Tetrahedron Lett.* **1983**, *24*, 5843-5846.
10. Kempe, T.; Sundqvist, W.; Chow, F.; Hu, S-L. *Nucleic Acids Res.* **1985**, *13*, 45-57.
11. (a) McBride, L.; Caruthers, M. *Tetrahedron Lett.* **1983**, *24*, 245-248. (b) Caruthers, M. *Science* **1985**, *230*, 281-285.
12. (a) Lokhov, S.; Podyminogin, M.; Sergeev, D.; Silnikov, V.; Kutyavin, I.; Shishkin, G.; Zarytova, V. *Bioconjugate Chemistry* **1992**, *3*, 414-419. (b) Serebryanyi, S.; Yufa, P. *Ukr. Khim. Zh.* **1963**, *29*, 322-325 (Russ.).
13. Kehrmann, F.; Havas, E. *Ber.* **1913**, *46*, 341-352.
14. Radner, F. *Acta. Chem. Scand.* **1983**, *B37*, 65-67.
15. (a) Sandström, A.; Kwiatkowski, M.; Chattopadhyaya, J. *Acta Chem. Scand.* **1985**, *B39*, 273-29. (b) Sandström, A.; Kwiatkowski, M.; Chattopadhyaya, J. *Nucleosides & Nucleotides* **1985**, *4*, 177-181.
16. Chattopadhyaya, J.; Reese, C.B. *Tetrahedron Lett.* **1979**, 5059-5062.
17. (a) Patel, D.; Kozlowski, S.; Marky, L.; Rice, J.; Broka, C.; Dallas, J.; Itakura, K.; Breslauer, B. *Bio chemistry* **1982**, *21*, 437-444. (b) Chu, Y.; Tinoco Jr, I. *Biopolymers* **1983**, *22*, 1235-1246. (c) Hunter, W.; Kneale, G.; Brown, T.; Rabinovich, D.; Kennard, O. *J. Mol. Biol.* **1986**, *190*, 605-618. (d) Hunter, W.; Brown, T.; Kneale, G.; Anand, N.; Rabinovich, D.; Kennard, O. *J. Mol. Biol.* **1987**, *262*, 605-618.
18. Hald, M.; Pedersen, J.; Stein, P.; Kirpekar, F.; Jacobsen, J. *Nucleic Acids Res.* **1995**, *23*, 4576-4582.
19. (a) Wagner, R.; Matteucci, M.; Grant, D.; Huang, T.; Froehler, B. *Nature Biotechnology* **1996**, *14*, 840-844. (b) Hodgson, J. *Nature Biotechnology* **1996**, *14*, 815-816.
20. Ebel, S.; Lane, A.; Brown, T. *Biochemistry* **1992**, *31*, 12083-12086.
21. Pachmann, U.; Rigler, R. *Exp. Cell. Res.* **1972**, *72*, 602-608.
22. Yamana, K.; Aota, R.; Nakano, H. *Tetrahedron Lett.* **1995**, *36*, 8427-8430.
23. Casale, R.; McLaughlin, L. *J. Am. Chem. Soc.* **1990**, *112*, 5264-5271.
24. Iwase, R.; Furutani, S.; Yamaoka, T.; Yamana, K.; Murakami, A. *Nucl. Acids Res. Symp. Ser.* **1996**, *35*, 117-118.
25. (a) Tesler, J.; Cruickshank, K.; Morrison, L.; Netzel, T. *J. Am. Chem. Soc.* **1989**, *111*, 6966-6976. (b) Tesler, J.; Cruickshank, K.; Morrison, L.; Netzel, T.; Chan, C. *J. Am. Chem. Soc.* **1989**, *111*, 7226-7232.
26. Ren, R.; Chaudhuri, N.; Paris, P.; Rumney, S.; Kool, E. *J. Am. Chem. Soc.* **1996**, *118*, 7671-7678.
27. (a) Asseline, U.; Delarue, M.; Lancelot, G.; Toulmé, F.; Thoung, N.; Montenay-Garestier, T.; Hèlène, C. *Proc. Natl. Acad. Sci.* **1984**, *81*, 3297-3301. (b) Fukui, K.; Morimoto, M.; Segawa, H.; Tanaka, K.; Shimidzu, T. *Bioconjugate Chemistry* **1996**, *7*, 349-355. (c) Fukui, K.; Tanaka, K. *Nucleic Acids Res.* **1996**, *24*, 3962-3967.
28. Koshkin, A.; Ivanova, T.; Bulychev, N.; Dobrikov, M.; Lebedev, A. *Bioorg. Khim.* **1993**, *19*, 570-582.
29. (a) Wiederholt, K.; Sharanabasava, R.; Giuliano Jr., J.; O'donnell, M.; McLaughlin, L. *J. Am. Chem. Soc.* **1996**, *118*, 7055-7062. (b) Sharanabasava, R.; Robles, J.; Wiederholt, K.; Kuimelis, R.; McLaughlin, L. *J. Org. Chem.* **1997**, *62*, 523-529.
30. Zhou, B.; Puga E.; Sun, J.; Garestier, T.; Hélène, C. *J. Am. Chem. Soc.* **1995**, *117*, 10425-10428.
31. Kwiatkowski, M.; Chattopadhyaya, J. *Acta Chem. Scand.* **1984**, *B38*, 657-671.
32. Chattopadhyaya, J.; Reese, C. *J. Chem. Soc. Chem. Comm.* **1978**, 639.
33. Welch, C.; Chattopadhyaya, J. *Acta Chem. Scand.* **1983**, *B37*, 147-150.
34. (a) Cashion, P.; Porter, K.; Cadger, T.; Sathe, G.; Tranquilla, T.; Notman, H.; Jay, E. *Tetrahedron Lett.* **1976**, *42*, 3769-3772. (b) Balgobin, N. *PhD Thesis*, **1982**, Uppsala.
35. Fasman, G. *Handbook of Biochemistry and Molecular Biology, Vol I*; CRC Press: Ohio. **1975**, p. 589.

(*Received in UK* 30 *April* 1997; *accepted* 29 *May* 1997)